Understanding the Dynamics of PRDM9- dependent and independent Meiotic Recombination Hotspots at the single cell level

A Thesis

submitted to

Indian Institute of Science Education and Research Pune in partial fulfilment of the requirements for the BS-MS Dual Degree Program

by

Asmita Bag

Indian Institute of Science Education and Research Pune
Dr. Homi Bhabha Road,
Pashan, Pune 411008, INDIA

Date: March, 2024
Under the guidance of
Supervisor: Dr. Corinne GREY
Institut de Génétique Humaine, CNRS, Montpellier, France
From August 2023 to February 2024

Certificate

This is to certify that this dissertation entitled ‘Understanding the Dynamics of PRDM9-dependent and independent Meiotic Recombination Hotspots at the single cell level’ towards the partial fulfilment of the BS-MS dual degree program at the Indian Institute of Science Education and Research, Pune, represents study/work carried out by Asmita Bag at *Institut de Génétique Humaine,* CNRS*,* Montpellier under the supervision of Dr. Corinne Grey, Deputy Director, IGH-CNRS UMR 9002, during the academic year 2023-2024.

(Dr. Corinne Grey)

Name of your Guide: Dr Corinne Grey

Name of Your TAC:

Dr Corinne Grey (Supervisor)
Dr Bernard de Massy (Co-supervisor)
Dr Mridula Nambiar (Expert Faculty Member at IISER Pune)

Committee: Department of Biology, IISER Pune

This thesis is dedicated to *my parents* and *my grandparents.*

Declaration

I hereby declare that the matter embodied in the report entitled ‘Understanding the Dynamics of PRDM9- dependent and independent Meiotic Recombination Hotspots at the single-cell level’ are the results of the work carried out by me in the Meiosis and Recombination Laboratory, *Institut de Génétique Humaine,* CNRS*,* Montpellier, France under the supervision of Dr Corinne Grey and the same has not been submitted elsewhere for any other degree. Wherever others contribute, every effort is made to indicate this clearly, with due reference to the literature and acknowledgement of collaborative research and discussions.

(Asmita Bag)
20191146

27th March 2024

Table of Contents

List of Figures

List of Abbreviations

AE:	Axial Element
ChIP:	Chromatin Immunoprecipitation
CE:	Central Element
DNA:	Deoxyribonucleic Acid
DSB:	Double Strand Break
DDSB:	Default Double Strand Break
dpi:	day(s) post injection
dpp:	day(s) postpartum
FE:	Functional Element
FISH:	Fluorescence *in situ* hybridisation
IF:	Immunofluorescence
IP:	Immunoprecipitation
KO:	Knockout
PAR:	Pseudo-Autosomal region
qPCR:	Quantitative Polymerase Chain Reaction
ssDNA:	single-stranded DNA
SSDS:	single-stranded DNA sequencing
WB:	Western Blot

Abstract

Meiotic recombination takes place in a specialised organisation of chromatin into loops and axes, which brings together the hotspots and the DSB forming machinery. In mammals such as mice, the location of the hotspots is tightly regulated by the meiosis-specific protein, PRDM9. However, even in the absence of this protein, breaks can be formed, which are redirected towards the default break sites (DDSBs) located at functional elements like promoters and enhancers, which also have H3K4 trimethylation epigenetic marks. Here, we try to provide a mechanistic understanding of how PRDM9 can efficiently recruit the DSB machinery proteins, such as MEI4 and the axis proteins, such as SYCP3, to the hotspots. To do so, we have set up a technique combining immunofluorescence and fluorescence *in situ* hybridisation (FISH) that allows us to track the hotspot and the DDSBs, along with the proteins MEI4 and SYCP3, in a single cell. Additionally, we also provide evidence for the genomic localisation of REC114, a component present in the same complex as MEI4.

Acknowledgements

At the start of embarking on this academic journey, I would like to express my gratitude to all the individuals whose valuable contributions have made the completion of this thesis possible.

First of all, I would like to thank my supervisor, Dr Corinne Grey, who introduced me to the topic and always encouraged me to delve deeper into it. Her patience and enthusiasm during all our discussion sessions made sure that I was more motivated afterwards, even when my experiments didn't go the way I expected them to. But I want to express my gratitude to her, especially for the support that she provided to me outside of the institute. Corinne, I am grateful to you and your family for welcoming me with open arms and helping me adjust to my life in Montpellier.

Next, I want to express my thankfulness to Dr Bernard de Massy, who believed in me and agreed to let me join his lab to do my thesis project. His guidance and encouragement helped me learn a lot about meiosis and recombination.

My heartfelt gratitude goes to Dr Mridula Nambiar, who kindly accepted the position of a member of my Thesis Advisory Committee.

To all my lab members, Christine, Fred, Isahak, Haruka, Paola, Lucie and Julie, who patiently guided me through my experiments and through my responsibilities in the laboratory. Of all of these people, I have to especially thank Christine for managing the lab duties and for providing help and resources to make sure that my experiments were on time, and to Lucie, who joined the lab during the last month of my internship and helped me both inside and outside the lab.

I would also like to thank the MRI team, the HR team and the people in Laverie at the institute who have extended their help, without which these six months would not have been such a smooth experience.

And finally, to people who have provided me with unwavering support even though they were miles away: my family and my friends. I don’t think I am exaggerating when I say that knowing that all of you believed in me has been my greatest source of inspiration. Your patience and understanding has been invaluable throughout the course of this journey.

Contributions

Contributor name	***Contributor role***
Dr Corinne Grey, Dr Bernard de Massy	Conceptualization Ideas
Asmita Bag, Christine Brun, Dr Corinne Grey, Dr Haruka Oda, Dr Frederic Baudat, Dr Bernard de Massy, Paola Sanna, Isahak Saidi	Methodology
Marie-Pierre Blanchard, Paola Sanna, Dr Haruka Oda, Dr Corinne Grey	Software
Dr Corinne Grey, Dr Bernard de Massy, Dr Frederic Baudat	Validation
Asmita Bag, Dr Corinne Grey, Lucie Fasolo	Formal analysis
Asmita Bag, Dr Corinne Grey, Lucie Fasolo	Investigation
Asmita Bag, Christine Brun, Lucie Fasolo, Dr Corinne Grey, Dr Mathilde Biot	Resources
Asmita Bag, Lucie Fasolo	Data Curation
Asmita Bag, Dr Corinne Grey	Writing - original draft preparation
Dr Corinne Grey	Writing - review and editing
Asmita Bag, Dr Corinne Grey	Visualization
Dr Corinne Grey, Dr Bernard de Massy	Supervision
Dr Corinne Grey	Project administration
Dr Corinne Grey, Dr Bernard de Massy	Funding acquisition

Introduction

1.1 Meiosis

Sexually reproducing organisms must undergo a specialised cell division called meiosis, which is crucial for the survival of their species. Meiosis consists of two rounds of cell division without any intervening step for the replication of DNA, ultimately generating four daughter cells or gametes. In each of these daughter cells, the genetic material is half of that of the parent cell, which gets restored after the fusion of haploid gametes during fertilization.

Meiosis, like mitosis, begins with DNA replication. The factor distinguishing the two is the so-called 'reductional division' in meiosis I, during which homologous chromosomes, and not sister chromatids, are separated. The segregation of maternal and paternal chromosomes into different cells reduces the genetic information present in the resulting cells, hence the name reductional division. The second round of cell division is similar to mitosis in that it separates the two sister chromatids (Petronczki et al., 2003) *(Figure1).*

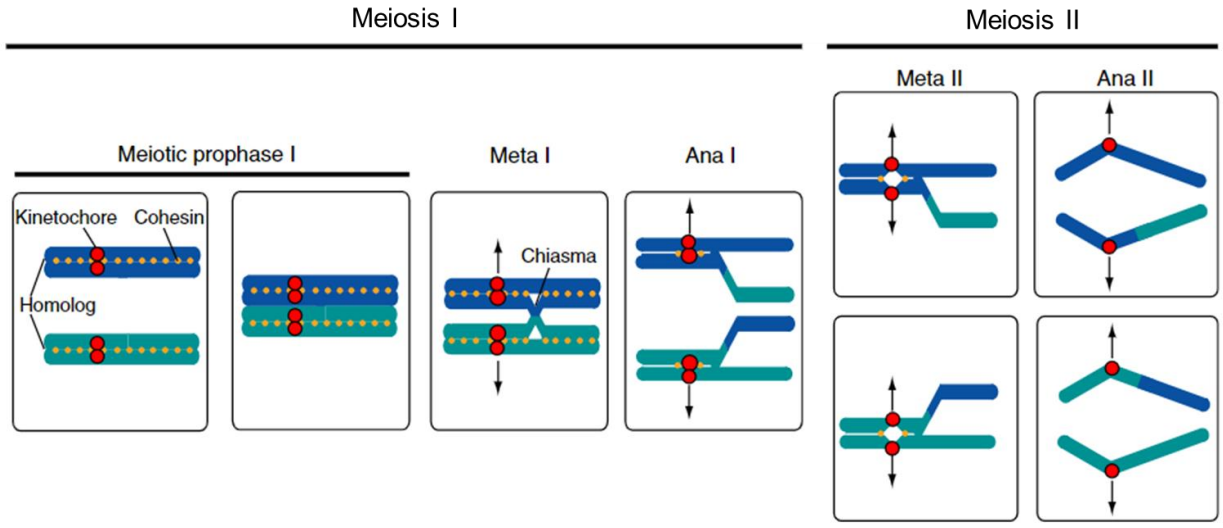

Figure 1: Stages of Meiosis: *During the first meiotic division, the homologous chromosomes are linked physically by the chiasma, which allows to satisfy the spindle assembly check point and ensures the proper segregation of the homologs into two daughter cells. In the second meiotic division, the sister chromatids separate, giving rise to four haploid daughter cells.*

To ensure that fidelity of homologous chromosome segregation is maintained, physical links must exist between them until the onset of anaphase I. These connections are provided by the reciprocal exchange of arms between one sister chromatid of each homolog, achieved through a homologous recombination event. These connections are cytologically seen as chiasmata (Zickler and Kleckner, 2015). Recombination between homologs not only allows the correct segregation of chromosomes but also increases genetic diversity by creating new allelic combinations. Failure in proper pairing of homologs can have dire consequences, such as gross chromosomal rearrangements or aneuploidy, which can lead to fertility issues and birth defects.

Stages of Meiosis I

Prophase of meiosis I is the longest stage in this nuclear division and is spread over several days. One prominent feature of prophase I is the extensive reorganisation of the chromatin into a specific loop-axis structure (Zickler and Kleckner, 1999). At the beginning of prophase I, the individual chromosomes start to condense, and the sister chromatids get attached to a proteinaceous structure formed by the axial elements (AE). Gradually, the homologs align with each other, and the two AEs on each homolog are ‘zipped up’ by the central element (CE). The AEs and the CE together compose the tripartite synaptonemal complex (SC), which plays an important role in the establishment, regulation and resolution of recombination events. According to the structure of SC, prophase I can be further divided into sub-stages (Page and Hawley, 2004; Petronczki et al., 2003) *(Figure 2).*

Leptotene marks the initiation of prophase I, where each homolog condenses into loops and is anchored to the axial element proteins. AE is formed by numerous proteins, the most prominent of which are cohesins, synaptonemal complex proteins - SYCP2 and SYCP3, and HORMA-domain containing proteins - HORMAD1 and HORMAD2. Under a light microscope, these proteins can be visualised as short stretches, and as leptotene progresses, the axis elongates.

It is during this stage that recombination is initiated by the introduction of hundreds of programmed double strand breaks (DSBs). These breaks are essential, as their repair by homologous recombination into non-crossovers (NCO) or crossovers (CO) promotes the search for homology to facilitate homologous pairing, and allows the establishment of physical connections between homologs.

At zygotene, the CE proteins are loaded and start to bridge the AEs. This brings the two homologous chromosomes together and initiates the formation of the synaptonemal complex, a process called synapsis.

During pachytene, the homologous chromosomes have fully synapsed, and the chromatin is now organised in a loop-axis arrangement. DSB repair is also completed during this stage with the formation of at least one crossover (CO) per homologous chromosome pair.

In males, even though the sex chromosomes are not identical (ChrX and ChrY), synapsis can take place in the short region of homology called the pseudo-autosomal region (PAR). This region covers approximately 700 kb from the distal end of the sex chromosomes and usually pairs late, towards the end of zygotene, when most of the autosomes have already been synapsed. Not just temporally, PAR DSB formation and repair are also genetically distinct from that of the autosomal chromosomes (Kauppi et al., 2012).

Throughout diplotene, the proteins of the CE get unloaded, and the synaptonemal complex is progressively disassembled. The homologous chromosomes separate except at the sites of reciprocal recombination (chiasmata). The last stage of prophase I is diakinesis, where the chromosomes condense further until the onset of metaphase I (Zickler and Kleckner, 1999; Page and Hawley, 2004; Morelli et al., 2008).

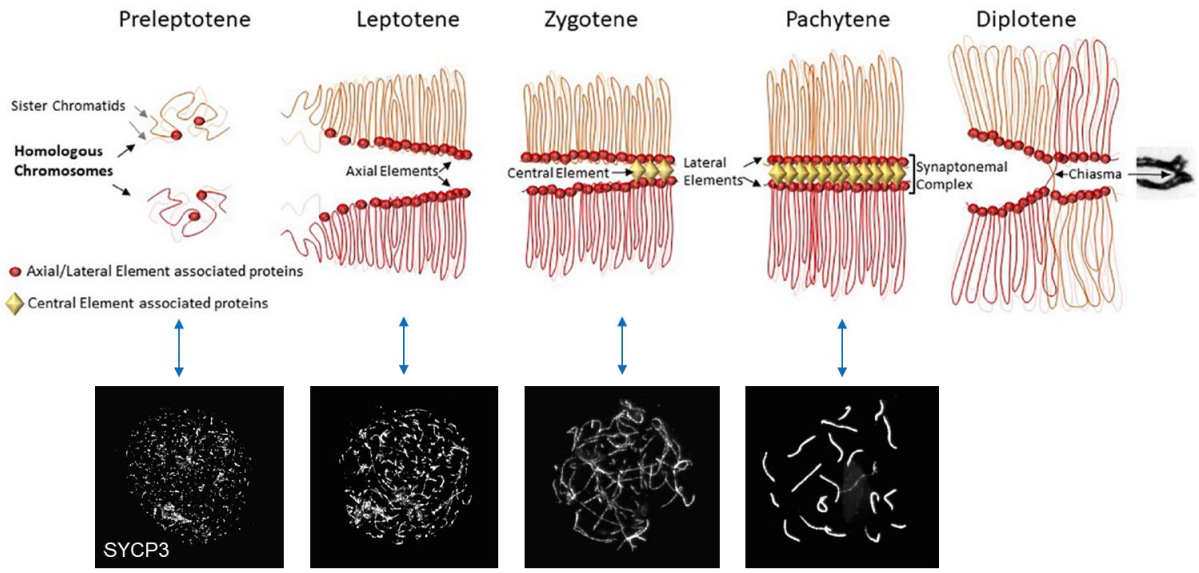

Figure 2: Schematic representation of the successive stages during Prophase I: *At the preleptotene stage, the axial element proteins are loaded on the chromosome. During leptotene, the axial element proteins come together to form an elongating structure where the loops get anchored. At zygotene, the central element proteins are loaded and act as a zipper to bring the two axes together to form the synaptonemal complex. In Pachytene, the homologs are fully synapsed, and the reorganisation into the loop-axis array is complete. During Diplotene, the synaptonemal complex is dissolved, and the homologous chromosomes are connected only via the chiasmata. Below each of these stages are the representative images taken using a widefield microscope.*

1.2 Mechanism of recombination initiation

Recombination during meiosis presents a great challenge to the cells. While it is arguably one of the most important steps, the presence of DSBs is also potentially detrimental. Thus, DSB formation and repair must be tightly regulated, both spatially and temporally, so that there is efficient crosstalk between the events taking place at the level of DNA and the chromosome organisation.

Soon after the meiotic S phase, DSBs are induced by the evolutionarily conserved protein SPO11, present in a complex with TOPOVIBL. The catalytic activity of SPO11 generates transient DNA-protein intermediates in which SPO11 remains covalently attached to the

5’ end of the breaks but eventually gets released by endo- and exo-nucleolytic cleavage. Following that, there is an end-resection, which creates a single-stranded overhang at the 3’ end on each side of the break. Single-strand binding protein RPA and then recombinase proteins RAD51 and DMC1 bind these ssDNA strands that can then promote strand invasion into duplex DNA to search for homology. On finding the homologous sequence, the break can be repaired by either of the two pathways: double Holliday junction (dHJ) pathway or synthesis-dependent strand annealing (SDSA) pathway. In the first pathway, the second DSB end undergoes capture to generate the dHJ structure, with its resolution predominantly leading to crossover recombinants. In the second pathway, the invading 3′ strand gets displaced after DNA synthesis, reanneals to the 3′ end of the DSB and is followed by additional DNA synthesis and nick ligation, ultimately producing non-crossover recombinant products (Kumar and de Massy, 2010; Lam and Keeney, 2015; Hunter 2015).

Proteins necessary for the formation of DNA double strand breaks

Although SPO11 is responsible for catalysing the breaks, it alone is not sufficient to form the DSBs. It is shown that Spo11 requires the presence of at least nine other proteins in *S. cerevisiae* for its meiotic DNA cleavage activity. Mutations in any of these proteins manifest as defects in the events of recombination initiation and spore unviability (Bergerat et al., 1997; Keeney et al., 1997). This highlights that these proteins together are responsible for the strict regulation of the formation of DSB to minimize any threat to the integrity of the genome.

In *S. cerevisiae,* these proteins can be assembled in three complexes: the core complex made of Spo11, Ski8, Rec102 and Rec104, the RMM complex (Rec114, Mei4, Mer2) and the MRX complex (Mre11-Rad50-Xrs2). The *in vitro* studies have shown the core complex to have a topology reminiscent of that of archeal TopoVI with Spo11 (Rec12 in *S. pombe)*, Ski8 (Rec14 in *S. pombe)*, Rec102 and Rec104 present in 1:1:1:1 stoichiometry. Further, the Rec102 and Rec104 proteins together form a complex in the budding yeast that is reminiscent of the TopoVIB subunit of the archaeal TopoVI.

The Mre11, Rad50, and Xrs2 proteins form a complex (MRX complex) together that has been well characterised in DSB processing because of the presence of exonuclease and endonuclease activities, but its role in DSB formation is not clear. The complex also has roles in vegetative cells, where it is implicated in DNA damage repair by both homologous recombination and non-homologous end joining (Keeney, 2001). The final complex is formed by the Rec114, Mei4 and Mer2 proteins (RMM), which localise to the chromosome axis. They form simultaneously with the synaptonemal complex, and their formation is consistent with the timing of initiation of meiotic recombination (Li et al., 2006).

The protein Spo11 present in the budding yeast is conserved in mice in terms of structure and function. The Rec102-Rec104 complex is also conserved to some extent in mice, as has been found by homology search. The TOPOIVB-like (TOPOVIBL) protein was shown to be an ortholog of the topoisomerase type B subunit VI of archaebacteria, similar to Rec102 and Rec104, and is required for the production of DSBs (Robert, 2016). The Ski8 orthologue, WDR61, has also been identified in mice, but no functional analysis on this protein has been done in mice to date.

The other two complexes, RMI (REC114-MEI4-IHO1 in *Mus musculus domesticus*) and MRN (RAD50-MRE11-NBS in *Mus musculus domesticus*) show a higher degree of functional and structural conservation across different taxa (Hunter, 2006; Cromie and Smith, 2008; Kumar and de Massy, 2010). The absence of specific homologs across species can imply that while the mechanism of DNA breaking might be the same, the regulation is completely identical and may have taken shape independently during evolution. The role of the proteins of the MRN complex can only be studied with hypomorphic mutants, as deleting any one of them leads to embryonic lethality. It has been shown that these proteins are essential during meiosis due to their involvement in the catalytical removal of SPO11 from the break ends and allowing end processing for DSB repair by homologous recombination, but might not have a function in SPO11-dependent DSB formation in mammals (Borde, 2007). The RMI complex, on the other hand, has an established function in break formation. Several studies have demonstrated

that they localise on the chromosome axis as foci at the onset of meiosis and help in the regulation of the activity of the TOPOVIBL catalytic complex (Kumar et al., 2010, 2018; Stainzione et al., 2016; Laroussi et al., 2023).

1.3 Localisation of Double Strand Breaks

Another aspect of the regulation of meiosis initiation is the localisation of DSB formation. Studies have shown that DSBs are not formed randomly across the genome but are more likely to occur in some parts than others. The regions on the genome with a higher-than-average frequency of DSB incidence are called 'hotspots', and regions with a lower-than-average frequency are called 'coldspots'. In *S. cerevisiae*, the hotspots occur in chromatin with open configurations marked by H3K4 trimethylation histone modification (Borde et al., 2009). On the other hand, for *S. pombe,* it has also been found that hotspots are more tightly associated with H3K9ac than H3K4me3 (Yamada et al., 2013). However, in both *S. cerevisiae* and *S. pombe*, hotspots occur in nucleosome-free regions.

In humans and mice, the meiosis-specific protein PRDM9 is responsible for specifying the sites for recombination initiation. PRDM9 has a C2-H2 zinc finger tandem array that confers binding specificity to hotspots *(Figure 3)*. It also has a SET-methyltransferase domain and can trimethylate H3K4 and H3K36 on nucleosomes near its binding site. These epigenetic marks can then be identified by components of the DSB initiation machinery and can promote DNA double strand break formation in those regions (Buard et al., 2010). The methyltransferase activity of PRDM9 is required for the formation of DNA DSBs at PRDM9 sites (Diagouraga et al., 2018). Furthermore, PRDM9 binding promotes local chromatin reorganisation through the eviction of nucleosomes, thus creating a nucleosome-free region.

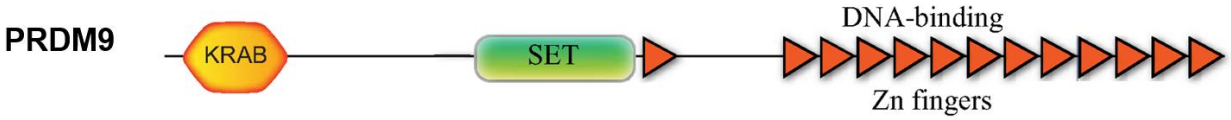

Figure 3: Schematic representation of the various domains present in PRDM9 protein. *PRDM9 has a KRAB domain, PR/SET domain and an array of zinc fingers (Source: Oliver et al., 2009 (modified)).*

Even though PRDM9 plays a crucial role in determining the localisation of hotspots, in its absence DSBs can still form. It has been shown that in mice lacking PRDM9, DSB formation is redirected towards H3K4me3-rich functional elements such as promoters and enhancers, much like what is observed in yeasts. However, breaks formed in *Prdm9KO* mice are not repaired efficiently and lead to infertility (Brick et al., 2012).

1.4 3-D architecture of the genome at the start of prophase I

S. cerevisiae remains one of the most extensively studied organisms to understand the initiation of recombination. The observations made in this model organism are indeed conserved across several kingdoms of life, including mammals. These studies have highlighted the important role of various proteins, like the cohesin complex(es), type II DNA topoisomerase, condensins and axis proteins, in the three-dimensional structure of the chromosomes (Grey and Massy, 2021).

The cohesin complex is made up of two coiled-coil proteins of the SMC (Structural Maintenance of Chromosome) family bridged together by a kleisin subunit and several accessory proteins. These accessory proteins can associate with the cohesin complex transiently to help with its loading/unloading to the chromatin. The four main subunits of cohesin during vegetative growth are Smc1, Smc3, Scc1 and Scc3. In meiosis, the kleisin subunit, Scc1, is replaced by a meiosis-specific paralog Rec8. Cohesins play a major role in chromatin organisation by bringing together sequences that are spread far apart on the linear chromosome, mediating contacts between different regions, likely trough loop extrusion (Peters et al., 2008; Nasmyth and Haering, 2009).

When the chromatin undergoes extensive reorganization into the loop-axis structure at the onset of Meiosis I, cohesin proteins form the base on these loops (Muller et al., 2018) and promote the recruitment of additional proteins such as the axis proteins Hop1 and Red1. The axis serves as a recruitment platform for other proteins such as the RMM (Rec114, Mei4, Mer2) complex, necessary for DSB formation. These RMM complex proteins can be visualized as distinct foci on the axial element. Surprisingly, it has been shown that hotspots in *S. cerevisiae* are located in the loops, which places them far away from the axis and, thus, the RMM proteins and the DSB forming machinery (Panizza et al., 2011). One model has been established in *S. cerevisiae* that proposes the tethering of hotspots, located within loops, to the DSB-forming proteins, located on the axis. Spp1 protein has been identified as the link between hotspots and the proteins present on the axis. Indeed, Spp1 is a component of the COMPASS complex that interacts with histone methyltransferase Set1 that catalyses H3K4 trimethylation, an epigenetic mark prominent at yeast promoters. By utilizing its PHD domain, Spp1 interacts with the H3K4me3 mark at promoters on one hand, and Mer2, a subunit of the RMM complex, on the other hand. This allows for the establishment of a connection between the RMM complex on the axis and the hotspots found in the loops (Acquaviva et al., 2013; Sommermeyer et al., 2013).

1.5 Need for this study

The link between the hotspots and the chromosomal axis, where the DSB forming proteins are found, has been identified in *S. cerevisiae* and proposed in *S. pombe*, but not yet in higher organisms like mouse. A recent study by Biot et. al (Molecular Cell, *in press*) under the supervision of C. Grey has addressed this gap in knowledge and has shown that in mice, the RMI proteins MEI4 and IHO1 also localise at the axis. However, differently to what has been reported in yeasts, hotspot localisation coincides with the axis proteins. This might simply reflect a change in the dynamics of axis formation relative to hotspot designation or underly a difference in the regulation of DSB formation in mammals compared to yeasts. Biot et al. also show that besides hotspots, CTCF sites and H3K4me3 enriched regions localise at the axis (and thus at the basis of loops). They suggest that the three types of sites, all loaded with proteins, might act as boundaries for loop extrusion and stall, at least for a while, at the basis of loops. This might provide

PRDM9-bound sites a window of opportunity to promote the efficient assembly of DSB-proteins, seen as distinct axis-bound foci, similar to condensates *(Figure 4).*

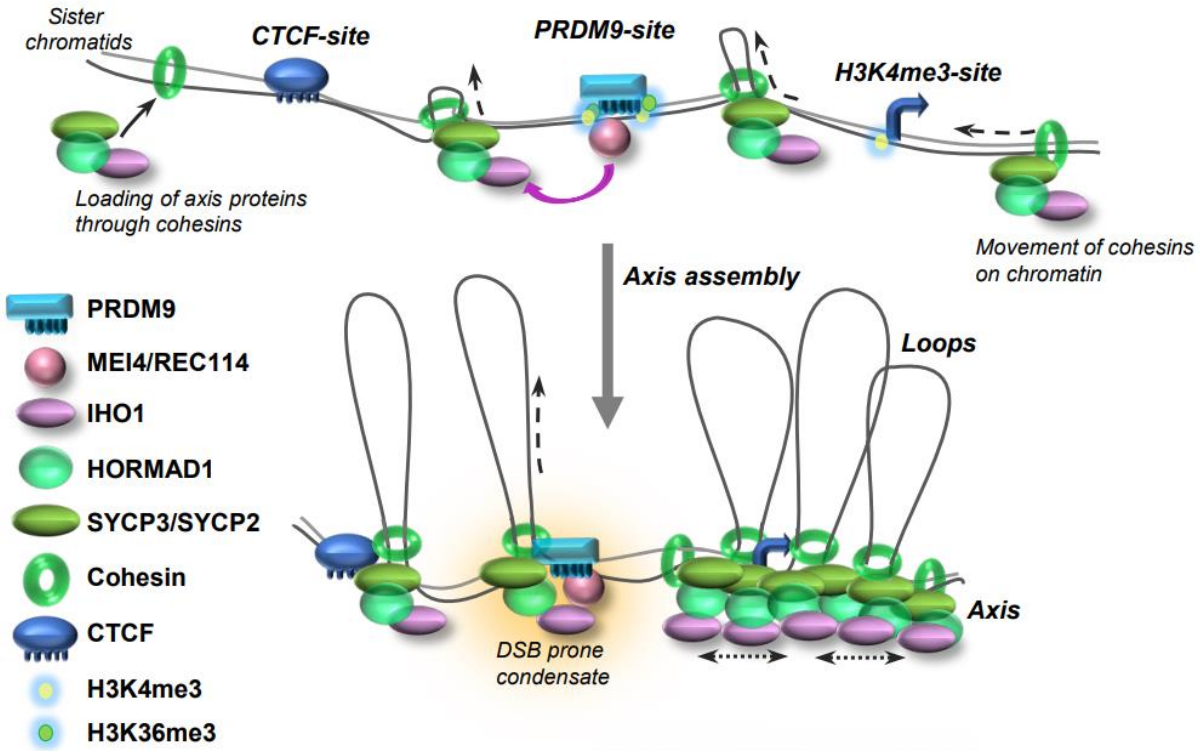

Figure 4: Schematic representation of the localisation of PRDM9 and the hotspot on the axis. *During meiosis initiation, cohesins aid axis protein loading on chromatin, and stabilise them at CTCF and PRDM9 sites enriched with H3K4me3, which act as barriers. PRDM9 sites at the base of the chromatin loops promote DSB formation protein condensate assembly.*

Interestingly, in *Prdm9* knockout mice, most recombination takes place at the promoters and other sites with H3K4me3 marks, such as gene-promoter regions and enhancers, called default double strand break sites (DDSB in this study) (Brick et al., 2012). Although in wild-type mice such sites are also enriched in H3K4me3, and they also localise preferentially at the axis (Biot et al., 2024), DDSB sites are seldomly used for the initiation of recombination when PRDM9 is expressed. But why would forming DSBs at promoters be problematic in mice, while in other organisms, such as yeasts or dogs, DSB formation

at promoters seems unproblematic? How is the DSB-machinery directed away from H3K4me3-rich DDSB sites to PRDM9-designated hotspots?

PRDM9 might be responsible for sequestering the recombination machinery from other H3K4 trimethylation sites on the genome. A possible scenario for the preferential use of PRDM9-sites is that PRDM9 enhances the efficiency of recruitment of DSB-machinery proteins to the axis. This heightened efficiency would facilitate rapid DSB formation and in turn promote axis formation, which has been shown to shut-down further DSB formation in a negative feed-back loop, preventing DSB formation at other sites. The sequestering of the DSB-protein machinery to PRDM9-sites, would further be enhanced if RMI proteins were present in limited amounts. Interestingly, even though the number of H3K4me3-rich sites largely exceeds number of available binding sites for PRDM9, in the absence of PRDM9, the number of MEI4 foci per cell remains stable, raising the possibility of a limited amount of protein.

In order to investigate more thoroughly the behaviour of DSB-machinery proteins in presence and absence of PRDM9, I want to investigate (i) the spatiotemporal dynamics of PRDM9-dependent hotspots and PRDM9-independent DDSB sites relative to the DSB-machinery protein MEI4 at the single-cell level and (ii) establish the genomic localisation (hotspot or DDSB site) of another RMI protein, REC114.

For the first project, I have adapted a method to visualise genomic loci (hotspots and DDSB sites) by fluorescence *in situ* hybridization, DSB-promoting proteins (MEI4) and axis proteins (SYCP3) by immunofluorescence simultaneously on a mouse spermatocyte chromosome spread. At the time of DSB formation, these players are supposed to come together, but it is interesting to observe their dynamics with respect to each other before break formation and compare how that can differ between hotspots and DDSB sites. In the end, this setup will also be used in mouse strains of different genetic backgrounds to get further insight into the interplay between the sites of break formation and the molecular players involved in the process.

Materials and methods

Spermatocyte chromosome spread preparation

Nuclei spread from the mouse testis was prepared as described by Peters et al., 1997.

Testis was taken from juvenile or adult mice and was placed in 200 µL of 1X PBS (500 µL for adults) after the removal of the tunica albuginea. Then, the testes were mechanically broken using scissors, and the suspended cells were homogenised further by pipetting up and down with a 200µl and a 1mL pipette, respectively. The cell suspension was then diluted by adding another 1mL of 1X PBS and set aside for 5 minutes to allow the cell debris to settle. After that, the supernatant was transferred to a new 1.5mL Eppendorf tube and centrifuged at 1459 rpm (or 200g) for 5 minutes at room temperature. All of the supernatant was removed except for 200 µL, and the pellet was resuspended in that. For adult mice, the cell suspension was transferred to a 15mL falcon tube after adding 1mL of 1X PBS, the cell debris was allowed to settle, and the supernatant was transferred to a new tube. The volume was then adjusted by adding 1X PBS to get a final volume of 10 mL. The falcon tubes were centrifuged at 1459 rpm (or 200g) for 5 minutes at room temperature; the supernatant was removed, leaving behind approximately 500 µL, which was then used to resuspend the pellet. This step was repeated two more times to end up with three washes to remove all of the spermatozoa, and the cells were counted.

An equal amount of hypotonic buffer (30 mM Tris-HCl pH 8.2; 50 mM sucrose; 17 mM sodium citrate; 5mM EDTA pH 8.0; 1X cocktail protease inhibitors (Roche); 0.5 mM DTT) was added to the cell suspension, and the tube was incubated for 8 minutes at RT and then centrifuged at 200g for 5 minutes at RT. For adults, the final volume was made up to 10mL by adding 1X PBS. The supernatant was discarded, and the pellet was resuspended in 1X PBS to have a concentration of 20 to 40 $\times$ 10^6 cells/mL. The slides that were to be used for chromosome spreads were dipped briefly in 1% Paraformaldehyde (1g of Paraformaldehyde in 100mL water and 250µL of 20% Triton

100X). A 1:2 ratio mix of cell suspension to 100mM sucrose was made, and 30µL was deposited on each slide. The slides were tilted slightly to spread the cells all over the slide and put inside a humid chamber for at least 1 hour or until the slides were almost dry. The slides were ultimately washed with 0.24% Photoflo (Kodak) and left to dry on a stand. Once completely dry, they were stored at -80℃.

Purification of MEI4 antibody

250µg of recombinant MEI4 was loaded onto a preparative 10% SDS PAGE gel within a single well, followed by electro-blotting onto nitrocellulose membrane, with the Biorad turbo system for 4 minutes. The blot was then stained with Ponceau Red for 5 minutes, and the portion containing the antigen was cut out and washed with distilled water or TBS1xTween (1%) (TBST) before being blocked with 5% Milk in TBST for at least 1 hour. After rinsing the strip twice with 10 ml of TBST, 3 ml of LavII P7 crude serum containing antibodies was added and incubated for 4 hours to overnight with constant shaking. The unbound fraction is poured off, and the strip is washed 3 times with 10ml TBST. Bound antibodies are eluted twice with 450 µl of glycine buffer (0.1M, pH 2.8) with vortexing for 5 minutes each time, followed by collection into a new tube and neutralization (pH 7.5) with 40 µl of 1M Tris pH 9.0. Additional elutions were performed with 400 µl of 50 mM glycine pH 1.9, incubated for 5 minutes each time, and the pH was neutralised with 100 µL of unbuffered 2M Tris. The concentration of the purified antibodies was determined by measuring the absorption of the sample at 280nm using the neutralized glycine buffer as blank, and the concentration (mg/ml) is calculated nanodrop quantification.

$$\text{Concentration (mg/ml)} = (1.55 \times A280) - 0.76 \times A260)$$

Immunofluorescence

The slides with the spermatocyte spreads were washed sequentially in 0.08% Photo-flo (Kodak) and 0.5% Triton 20x (Sigma). A milk-based blocking buffer was prepared using 5% milk and 5% donkey serum in PBS 1x. The blocking buffer mixture was centrifuged at 15000 rpm for 10 min, and the supernatant was collected and stored at -20˚C. 100µL

of the buffer was applied to the slides at room temperature for 30min. Primary antibodies used were rabbit anti-MEI4 (1:100, homemade - Lav8 II 2020) and mouse anti-SYCP3 (1:300; Abcam 97972). The primary antibody solution was prepared in the Can Get Signal™ Immunostain solution B (TOYOBO, NKB-401), and incubation was performed for 1 hour at room temperature. The unbound primary antibody was removed by sequential washes in Photoflo and 20% Triton 100X, followed by another round of blocking. Secondary antibodies were donkey anti-rabbit Alexa Fluor 488 (1:300; Life Technologies, A21206) and donkey anti-mouse Alexa Fluor 555 (1:300; Abcam 150110). Secondary antibody solution was prepared in the Can Get Signal™ Immunostain solution B (TOYOBO, NKB-401) and incubation was done at 37˚C for 90 min. After the secondary antibody was washed off with 1X PBS for 5 minutes twice, fixation was done with PFA2% in 1X PBS for 10 minutes at RT. The fixing solution was washed off by washing the slides in 1X PBS twice at RT before taking the slides ahead for FISH.

Fluorescence in situ hybridization

Slides containing chromosome spreads from mouse testis were washed with 0.08% Photo-flo (Kodak) twice and treated with 100 µg/mL RNAse A prepared in SSC 1x (saline sodium citrate) solution at 37˚C for 30 min to 1 hour. The RNAse was washed off by dipping the slides in SSC 1x solution and covered with 100µL 50% formamide/50% SSC 2x and kept at RT for 20 minutes. The slides, along with the solution of formamide/SSC was transferred to 60˚C for another 20 minutes. These slides were then put on a heating block calibrated at 85˚C for 5 minutes to denature the DNA, immediately washed with ice-cold SSC 2x and dried. The hybridization solution was prepared by mixing 50% formamide, SSC 2x solution, 10% dextran, 2.5µg of mouse Cot1-DNA (Invitrogen), 10µg of sheared salmon sperm DNA (Invitrogen) and probe (50ng), and denatured at 93˚C for 3 minutes. 15 µL of the solution was applied to the slides, covered with a coverslip, and sealed with rubber cement. The slides were incubated overnight in a humid chamber at 52˚C. The next day, the rubber cement was peeled off, and the slides were washed in SSC 0.05x solution at 60˚C for 10 minutes, followed by two washes in SSC 0.05x solution at RT. After this, nuclei were stained with 1x DAPI (4′,6-diamidino-2-phenylindole). The

DAPI stain was washed off by briefly dipping the slides in water. The slides were dried on a rack, and mounting was done using Prolong Gold (Invitrogen).

Fluorescence microscopy image acquisition

The images were obtained using a Zeiss Axioimager Z3 microscope.

Chromatin Immunoprecipitation

Chromatin immunoprecipitation (ChIP) experiments were conducted using the ChIP-IT High Sensitivity kit from Active Motif (53040), with slight modifications to the manufacturer's instructions. Chromatin was prepared from snap frozen synchronized testes at 8dpi. Four synchronized testes, without the tunica albuginea, were homogenized in a 15 mL douncer with a tight-fitting pestle (Type A) (~20 strokes) and fixed at the same time in the fixation buffer (according to the manufacturer's instructions) for 15 min at RT. Following quenching of the reaction with Stop Buffer, the cell suspension was washed and lysed as directed by the manufacturer. Nuclei suspensions were sonicated in a 15 mL Falcon tube containing 1.5 mL of lysis buffer using a Qsonica sonicator with the following settings: 30 seconds ON, 30 seconds OFF, for a total of approximately 3 minutes and 50 seconds ON time, reaching a cumulative energy of 2,000 Joules (15% power). After sonication, the chromatin was concentrated to a volume of 1 ml using a Vivaspin column, and 25 µl was set aside as input control for analysing shearing efficiency and chromatin quantification.

IPs were performed with 30-40 µg of chromatin and with 4µg of antibody as recommended by the manufacturer's instructions. The following antibodies were used: anti-SYCP3 (Abcam; 15093), anti-MEI4 (homemade – L8 E1 2020), and anti-REC114 (homemade – serum 037 G beads).

Results and Discussion

PART I

In the mouse, DSB sites can be identified and mapped by using chromatin immunoprecipitation followed by sequencing (ChIP-seq) against the DMC1 recombinase. This technique has allowed the identification of over 18,313 hotspots in the laboratory mouse strain C57BL/6, expressing PRDM9^{Dom2} (Khil et al., 2012), and almost 30,000 DDSB sites in C57BL/6 lacking PRDM9 (*Prdm9KO*) (Brick et al., 2012). To analyse how hotspots and DDSB sites behave at the onset of prophase I, we aim to answer two questions: where are hotspots and DDSB sites located within the higher-order chromatin organisation, and when and how do they interact with the RMI proteins and axis proteins.

Fluorescence *in situ* Hybridization (FISH) assay on chromosome spreads will allow us to look at hotspots and DDSB sites in space at the single cell level. When this technique is combined with immunofluorescence, the assay will allow us to look at the relation between DSB sites, chromosome axis and RMI proteins. The combined technique, referred to as Immuno-FISH in this text, has been performed on chromosome spreads prepared from the testis of 16-17 days postpartum (dpp) mice. Male mice start producing sperm from 8 dpp, and continue to do so every 8-9 days during their lifetime, allowing a constant production of sperm cells. During the first wave of meiosis, where spermatogonia stem cells start differentiating to form sperm, only a specific cell stage will be present in the testis in the majority. Using testis from mice aged 16 or 17 dpp, allows us to simultaneously observe a significant amount of pachytene spermatocytes originating from the first wave of spermatogenesis and early stages (Leptotene/zygotene) originating from the second wave.

3.1 Designing the probes

To assess the localisation of hotspots and DDSB sites, I first had to choose a subset of genomic loci containing candidate sites. As assessed by DMC1 focus count (Immunofluorescence), reflecting break sites at the single cell level, out of the roughly 20,000 to 30,000 potential sites, only about 200-500 hotspots or DDSB sites are used within a single nucleus. To study an eventual colocalization between one of those sites and the DSB-machinery or the axis, it is thus crucial to carefully select highly used sites, which show a strong enrichment in DSBs and DSB-machinery proteins as assessed in population-based ChIP-seq assays. The genomic localization of DMC1 (reflecting break sites), MEI4 and IHO1 - the RMI proteins (reflecting the DSB-machinery) and SYCP3 and HORMAD1 - the axis proteins binding to hotspots and DDSB has been mapped by ChIP-seq (Brick et al. 2012; Biot et al., 2024). This allowed me to select sites with a robust binding of all those markers. I thus compared the DMC1 ChIP signal on the Integrated Genomic browser with the ChIP signal for MEI4, IHO1, SYCP3 and HORMAD1 in the wildtype and in *Prdm9KO (Figure 5).* I looked for hotspots and DDSB sites with strong enrichment for DMC1 protein and consistent enrichment for at least one RMI protein and one axis protein. Based on these criteria, I selected a subset of 24 hotspots and 26 DDSB sites.

After selecting the loci containing the candidate hotspots or DDSB sites, I set out to design FISH probes for each individual region. We chose an approach where FISH probes are produced from PCR fragments covering the region of interest, and then marked with a fluorophore. For that, first we had to design specific primers that amplify the fragment containing the region of interest with a minimal number of repetitive regions, to avoid off-target binding and non-specific background noise. The sequence of a given locus was obtained from Integrated Genome Browser 9.1.10 and masked for repeats using RepeatMasker. In the end, among the 24 shortlisted hotspots and 26 shortlisted DDSBs, I selected four sites with minimal amounts of repetitive sequences, two hotspots and two DDSB sites. These four loci were named based on the chromosomes where they are located: the two hotspots are called Chr8 and Chr17, and the two DDSB sites are called

Chr4 and Chr8. For each of the four sites, 7-8 pairs of primers were designed on the 10kb-interval, with each pair producing an amplicon of about 1 kb, allowing a probe that covers a total region of about 7 to 8kb at or flanking the candidate DSB site. To ensure more stringent quality control for the primers and, ultimately, the probes, all the primer pairs were used to run a PCR simulation to verify whether they generated exactly one amplicon. The ePCR-generated amplicon was then used as input for NCBI BLAST to check for similar sequences present on the mouse genome.

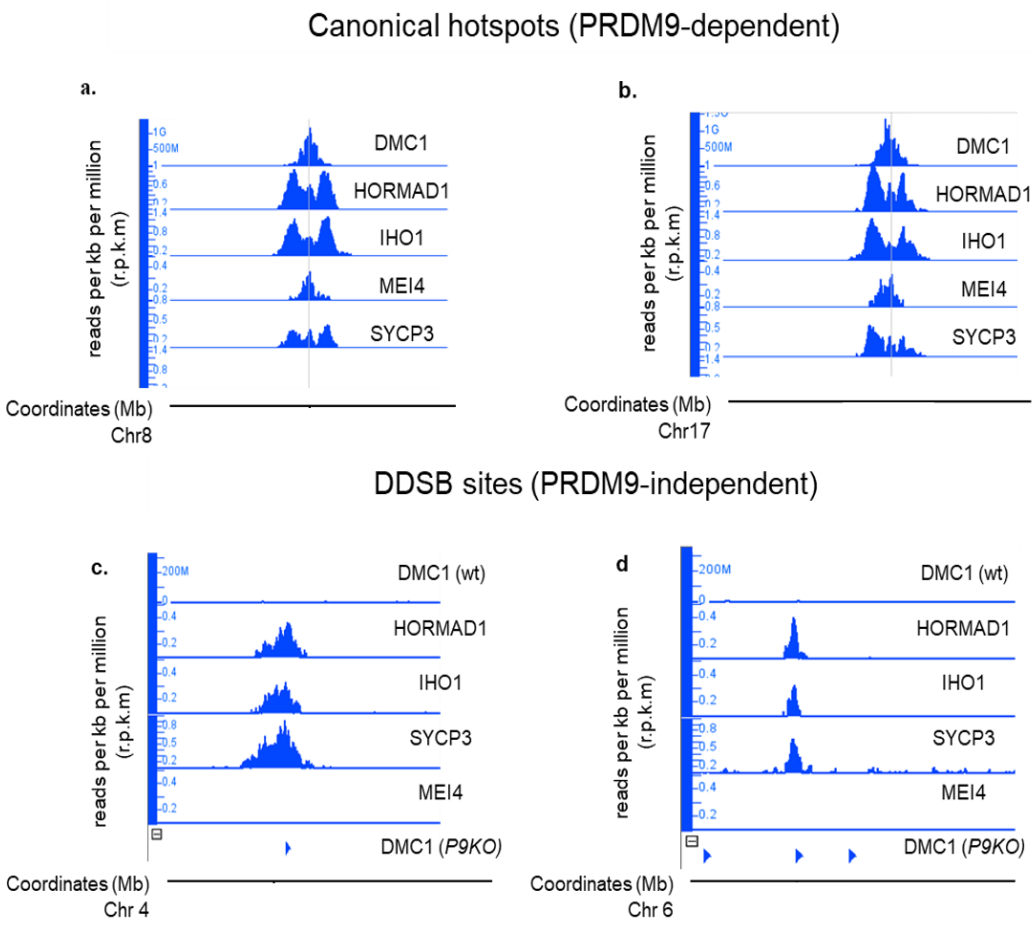

Figure 5: Snapshots of Integrated Genome Browser images showing the read enrichment of DMC1 recombinase, HORMAD1 and SYCP3 axis proteins and IHO1, MEI4 RMI complex proteins at four distinct genomic loci. *(A) and (B): PRDM9-dependent hotspots in the B6 genome (wild type); (C) and (D) PRDM9-independent hotspots in the B6 genome (Prdm9KO) – the DMC1 signal in the Prdm9KO mice are shown in .bed format which only highlights the statistically significant DMC1 peaks.*

3.2 Amplification the break sites to make the probes

Genomic DNA from C57BL/6 was used to amplify the DNA which will be further used to make the probes. After the first PCR, the samples were run on a 2% agarose gel, where bands other than the expected band size also showed up. To get rid of these non-specific bands, and to maintain the purity of the probe to be made downstream in the process, the band corresponding to the expected size was cut out and purified by gel extraction *(Figure 6)*. The gel-purified product was once again used to run another PCR with the same conditions as the first one and purified again to obtain DNA without any salt contamination *(Figure 7).*

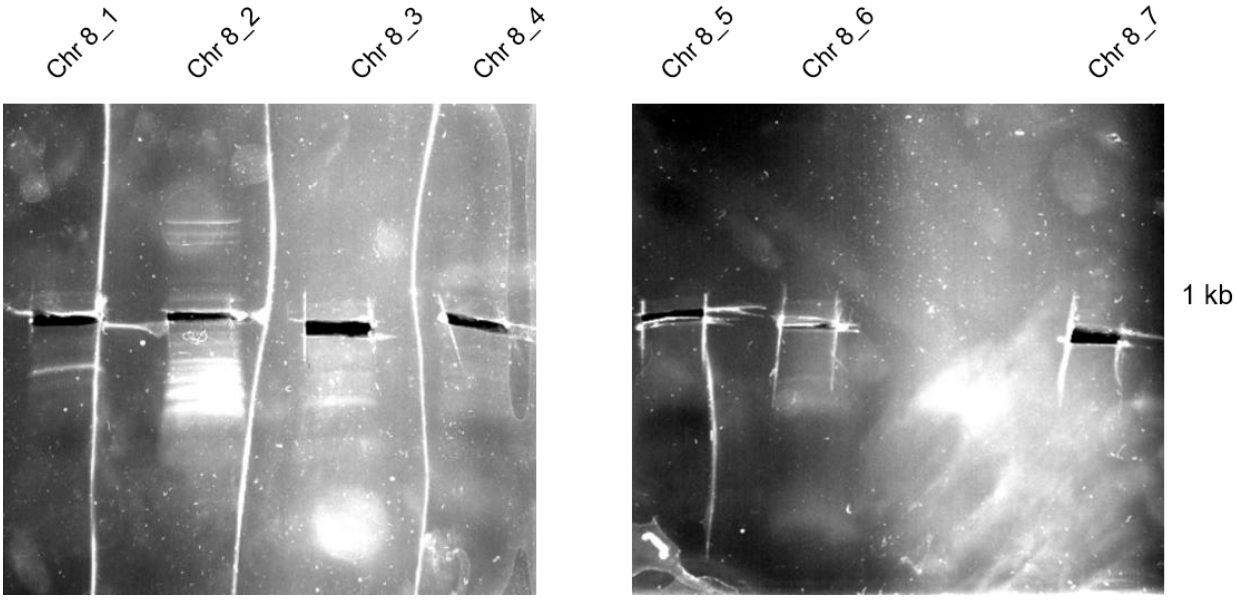

Figure 6: Gel from which the amplicon with the expected band size was cut out. To reduce the damage to the DNA due to UV exposure, the bands were excised under bright blue light, and then images were captured using UV light.

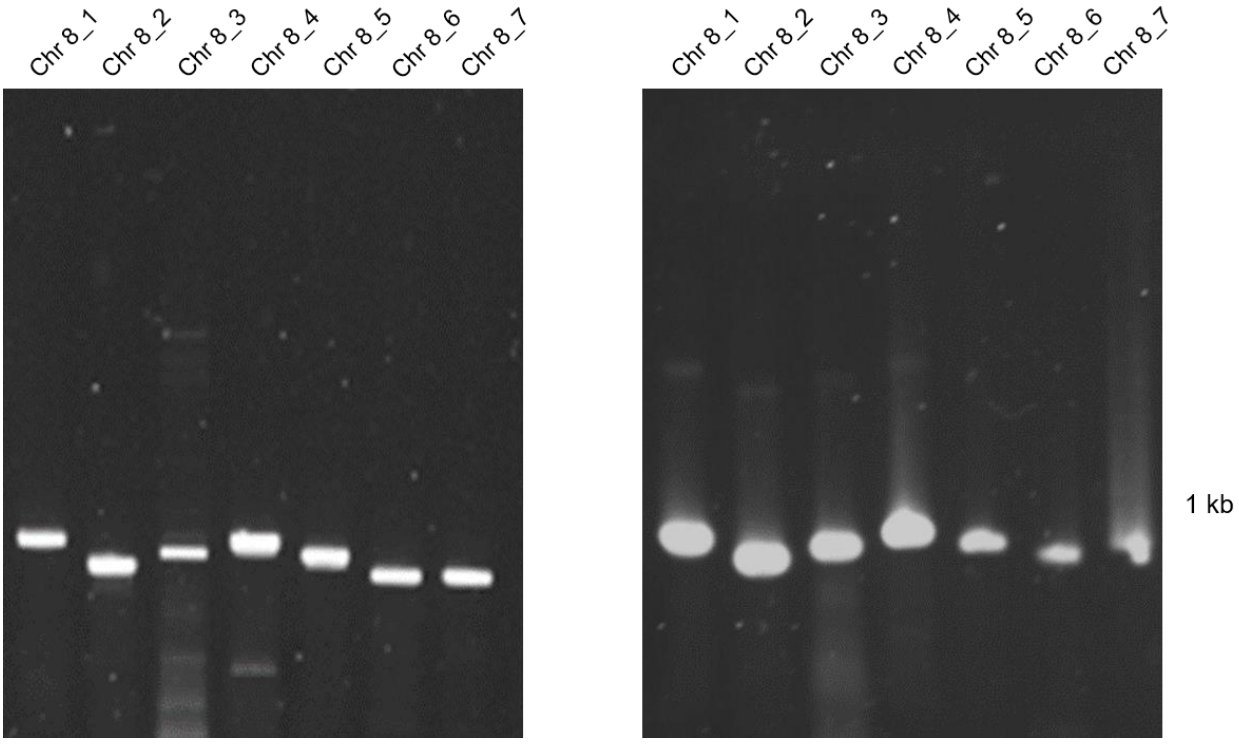

Figure 7: Gel with the amplicon to be used for the FISH probes. The gel on the left: The first PCR (before Gel extraction of the desired band); gel on the right: The second PCR with the gel-purified product as the template (after Gel extraction of the desired band)

3.3 Tagging the probes with fluorophore

The probes were prepared as per the directions of the manual of FISHTag kit (Invitrogen). The probes are produced in two steps. In the first step, the aminoallyl dUTP is incorporated into DNA using nick translation. Next, the resulting amine-modified nucleic acid is labelled using the amine-reactive dye provided with the kit *(Figure 8).*

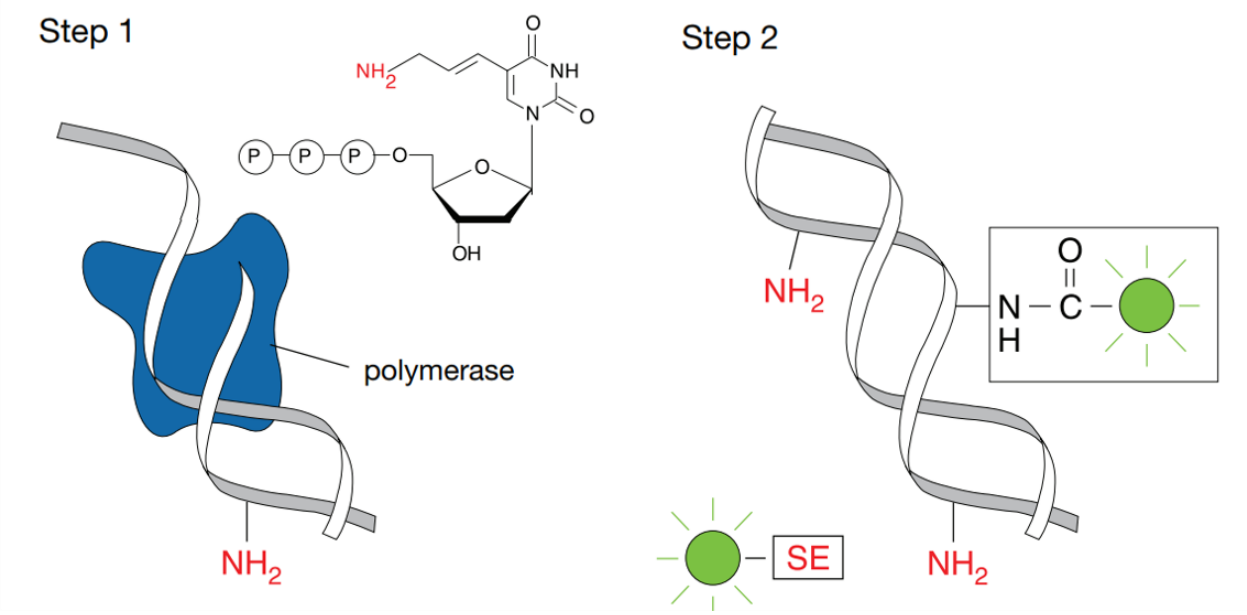

Figure 8: Schematic diagram of the labelling method used for tagging the probes with fluorophore. *The FISH Tag™ DNA uses a two-step method to label DNA. Step 1) The aminoallyl dUTP is enzymatically incorporated. Step 2) A reactive fluorophore is used to label the incorporated aminoallyl group (Source: The Molecular Probes® Handbook: A Guide to Fluorescent Probes and Labeling Technologies, 11th edition, 2010)*

An equimolar mix of all the fragments for one probe was prepared and digested with the DNAse I nick translation mix. To find out the optimal time for digestion that would generate bands between 300-700 bp, I conducted a time course experiment. A fraction of the digested DNA was taken out of the tube at 30-minute intervals and vortexed to inactivate DNAse I enzyme and deposited on a 2% agarose gel for migration *(Figure 9).* However, this proved to be insufficient at completely inhibiting the digestion reaction, so the samples

were stored at -20°C immediately after vortexing before running all the samples on a 2% agarose gel simultaneously.

Through numerous trials, I selected the optimal time for digestion to be 1 hour for all four probes. This produced fragments with average size of 300bp, a size within the desired range for optimal hybridisation.

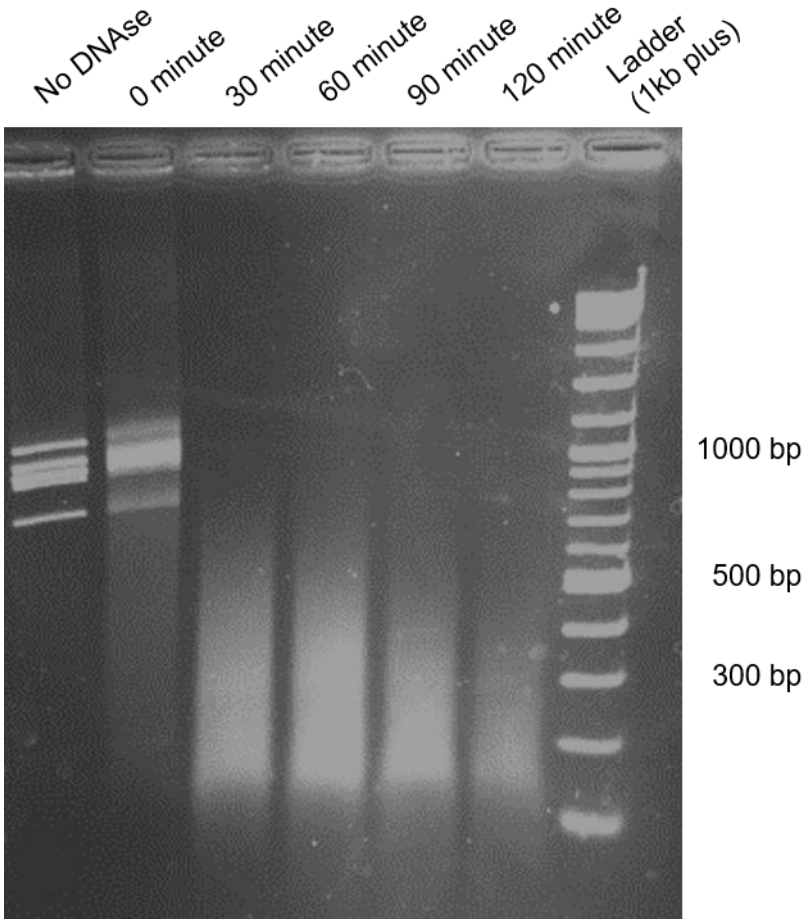

Figure 9: Time course experiment for calculating optimal digestion time for probe preparation. *As soon as we add the DNAse I nick translation mix, the digestion of DNA starts. At one hour time point, the bulk of the digested DNA is around 300 bp. To obtain probe with optimal labelling, we want the bulk of the digested DNA to lie between 300-700 bp.*

The DNAse I digested product has incorporated modified bases by nick translation reaction. In the next step, we introduced the fluorophore, which can bind to the modified base and give out fluorescence when exposed to light with the corresponding excitation wavelength.

The degree of labelling (number of dyes incorporated per 100 bases of the probe) was calculated using the following equation:

$$\#\ dyes/100\ bases = \frac{100}{(A_{base} \times \varepsilon_{dye})/(A_{dye} \times \varepsilon_{base})}$$

For labelling with Alexa Fluor 555, I typically retrieved probes with 1-3 pmol/µL of the dye and for labelling with Alexa Fluor 488, I typically retrieved probes with 2.5-5 pmol/µL of the dye.

3.4 Setting up Immunofluorescence and FISH

We want to set up the protocol that will allow us to obtain robust signal for the hotspots or the DDSB sites by FISH, and let us simultaneously observe the localisation of the proteins MEI4 and SYCP3. We, therefore, had to find the ideal conditions to combine FISH with immunofluorescence. As a starting point to set up this technique, I decided to start with a protocol that was already used in our lab to hybridise BAC (Bacterial Artificial Chromosome) probes. However, BAC FISH probes cover loci exceeding 250kb, rendering them more compatible with diverse conditions compared to PCR probes. Therefore, I needed to assess whether the protocol combining immunofluorescence and FISH with BAC probes, presented as a flowchart below *(Figure 10)*, was also suitable for the PCR probes and antibodies that I intended on using.

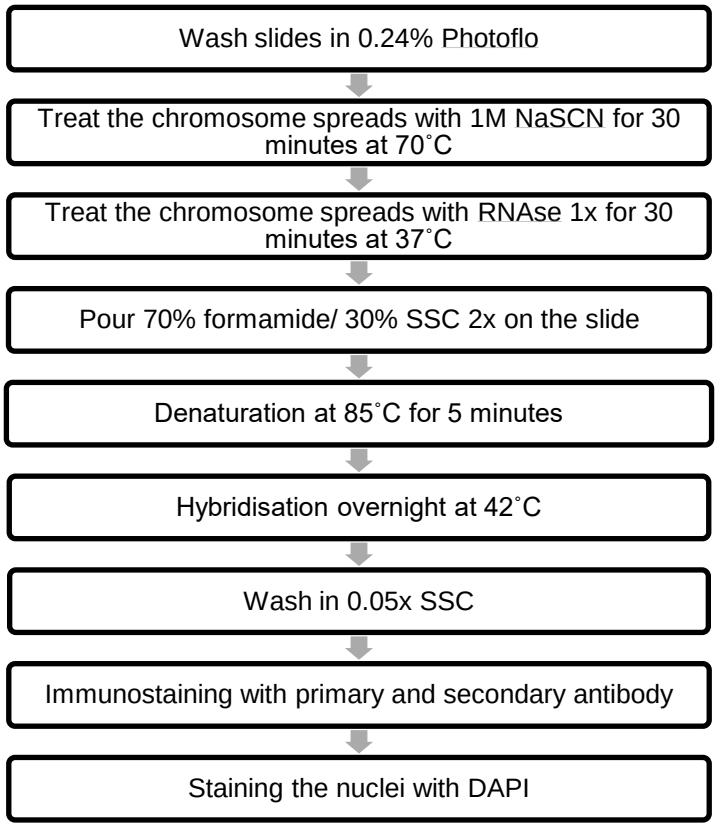

Figure 10: Workflow for the current Immuno-FISH technique. *The slides with the chromosome spreads were taken out of -80˚C and washed with Photoflo. Then they were treated with NaSCN and RNase respectively. The slides were then covered with 70% formamide/ 30% SSC 2X, and placed on a heating block for denaturation. The probe was then added and allowed to hybridise overnight. At last, immunostaining was done and the nuclei was stained with DAPI.*

To do that, I performed only an immunofluorescence (IF) experiment, without it being followed by FISH. The IF was performed on spreads from 16*dpp* mice, and the antibodies used were anti-MEI4 and anti-SYCP3. Through this, it was verified that the antibodies indeed worked well for the conditions that we had set for IF. MEI4 and SYCP3 localisation followed the expected pattern in leptotene, zygotene and pachytene. In leptotene, SYCP3 and MEI4 both showed up as foci under the microscope and co-localised. In zygotene, we observed that, SYCP3 was no longer seen as foci but was visualised as long stretches, with the length depending on how far the cell has progressed through zygotene.

At this stage, MEI4 was localised on the axis. In pachytene, when the axis has fully synapsed, SYCP3 was still visible as a long stretch, but MEI4 mostly disappeared from the cell. However, some MEI4 signals were still retained, although they were not localised on the axis anymore *(Figure 11).*

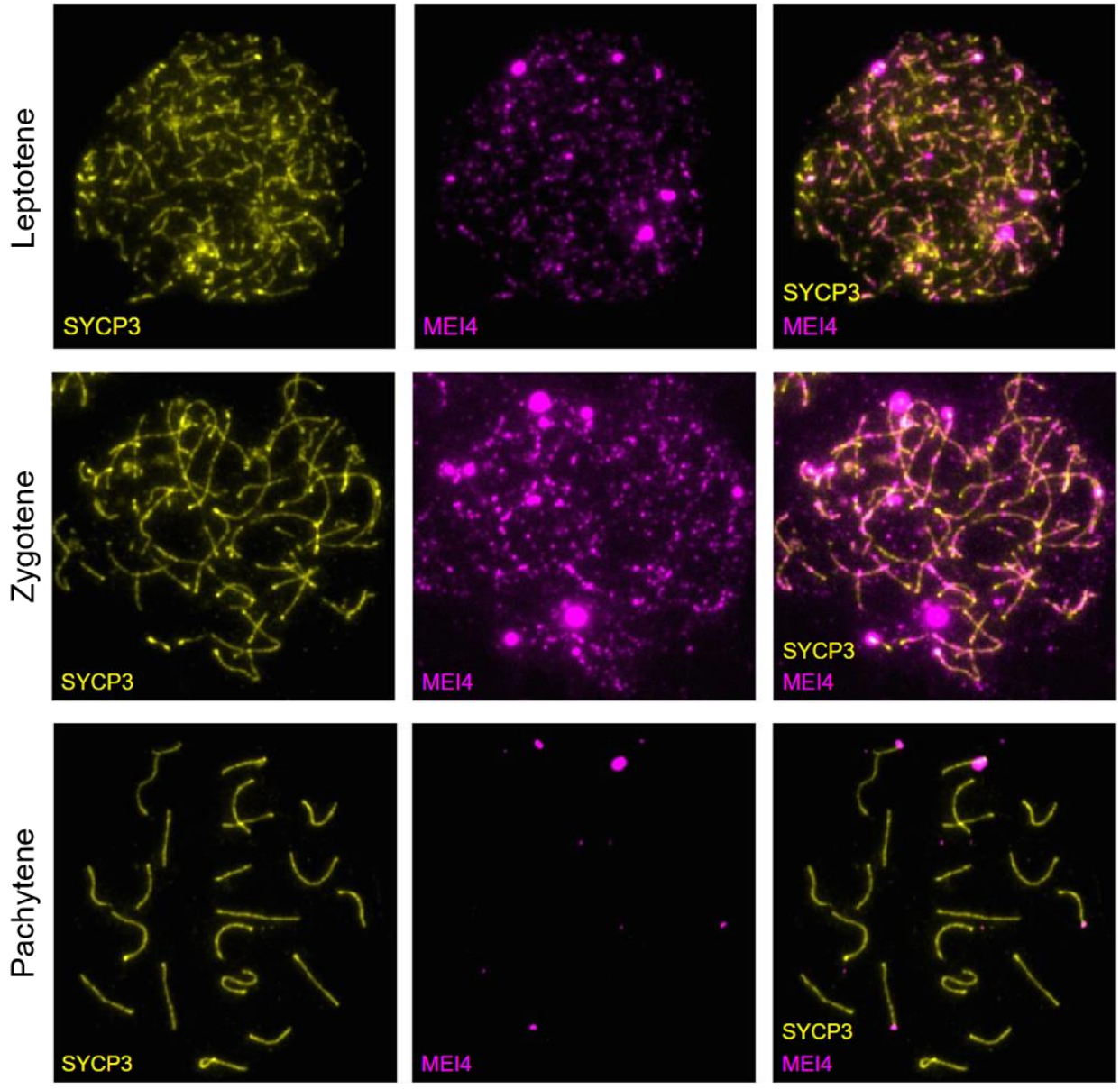

Figure 11: MEI4 and SYCP3 in mouse testis. *MEI4 co-localises with SYCP3 on unsynapsed axis but disappears as synapsis takes place.*

Next, I started testing the combination of the FISH protocol with RMI and axis protein immunostaining. While preparing the new probes that I designed, I performed tests with the *Psmb9* hotspot probe, which had already been prepared before my arrival. The *Psmb9* hotspot is a control for our experiments, because this hotspot is activated by the *Prdm9*^{Cast} allele and thus not functional in the C57BL/6 mouse strain, expressing *Prdm9*^{Dom2} allele.

With this probe, covering a single locus of about 7kb, it is expected that between one to four foci can be observed per nucleus, corresponding to the four sister chromatids present in meiotic spermatocytes. In my experiment, a few foci which can likely correspond to *Psmb9* signal can be detected *(Figure 12),* but the results were not consistent in all nuclei. Indeed, some nuclei yielded more foci, which were probably due to non-specific binding.

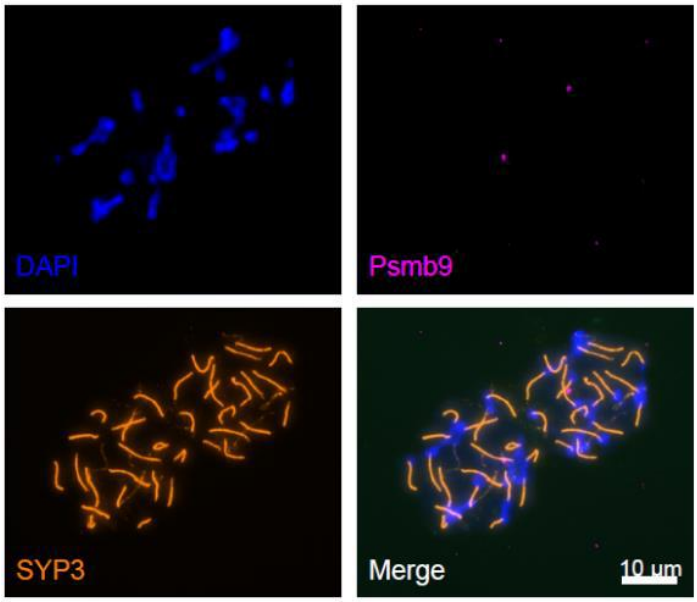

Figure 12: Immuno-FISH experiments on chromatin spread of B6 mouse spermatocytes. *(A)Upper left panel DAPI staining (blue), upper right panel: Psmb9 FISH probe staining (pink), Lower left panel: SYCP3 axis protein staining (red), Lower right panel: merge of the three colours.*

This showed that the conditions, although ideal for IF, were not ideal for Immuno-FISH. Thus, we needed to optimise the current protocol so that a reliable signal could be detected from the hotspot or the DDSB. DNA FISH has five major steps: (i) Pretreatment of the chromatin to make it more accessible for probe and antibodies, (ii) RNAse treatment to ensure that all ssRNA are removed and the probes cannot bind non-specifically to them, (iii) Denaturation to generate ssDNA for the probe to bind to, (iv) Hybridization of the probe and the target, and (v) Post-hybridization washes to remove all unbound probes from the sample to get robust signals on imaging (Figure 12). In addition to these five major steps, the combined protocol of Immuno-FISH has another important aspect - the order of IF and FISH. I have optimised some of these steps, which has led to robust signals from both the proteins (MEI4 and SYCP3) and the probe, and this is described in detail in the following sections.

3.4.1 Sequence of IF and FISH

To complete the FISH protocol, the chromatin must be exposed to high temperatures during the denaturation process. This harsh treatment is likely to affect epitopes of some proteins such as MEI4, in turn affecting its immunodetection. One way to get around this is to perform IF first and fix the slides before performing FISH. The fixing was done using 2% PFA (see Materials and Methods), and then FISH was performed. We can observe that, while the staining of SYCP3 did not really change, better signal was retrieved for MEI4, specially at zygotene *(Figure 13).* In addition, there was less background in the regions surrounding the nucleus for the channel used to visualise MEI4. However, these two tests did not produce drastically different results, and I need to look at more cells before I can arrive at a conclusion from this test. I also need to look at other conditions involved for a successful Immuno-FISH experiment, and as there is no severe change, I will still have the possibility to do first FISH and then IF.

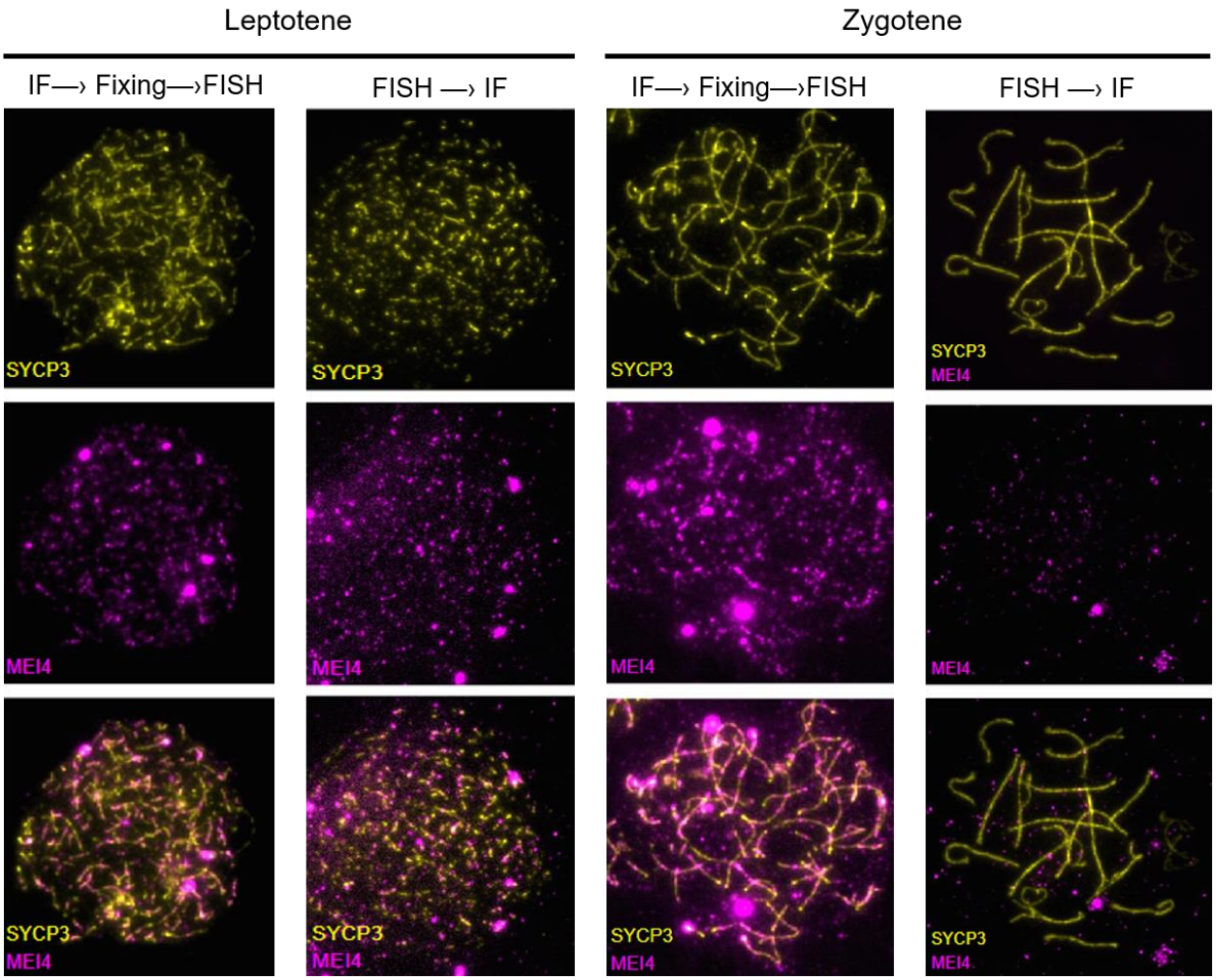

Figure 13: Different stages in mouse sperm formation highlighted by MEI4 and SYCP3. *First two panels- Leptotene. MEI4 signal in the leptotene stage shows better co-localisation with SYCP3 in the condition where IF is performed before FISH. Last two panels - Zygotene. SYCP3 in yellow and MEI4 in Magenta*

3.4.2 Pretreatment of the nuclei during FISH

The pre-treatment stage is one of the first steps during FISH assay. In the initial version of the FISH protocol, this step was performed with NaSCN (Sodium thiocyanate) to reverse the crosslinking between proteins done during chromosome spread preparation and to allow better penetration of the probes, all the while preserving the morphology of

the cells. However, NaSCN is very harsh on cells and can result in the degradation of our protein of interest, MEI4. To avoid that, I wanted to try a less harsh solution for pre-treatment, Citric acid buffer, which has been validated for FISH by Oliver-Bonet, 2009. Moreover, I wanted to test if pre-treatment was even necessary for the binding of probes.

In Figure 14 below, we can observe that for the condition where no pre-treatment has been performed, the background signal for the probe is less prominent when compared to the two other conditions, pre-treatment using NaSCN, and Citric acid buffer (CAB). Between the two different conditions for pre-treatment, treatment with CAB at 80°C for 1 hour is slightly better in terms of background signal than NaSCN at 70°C for 30 minutes, and is comparable to the condition of no pre-treatment. However, all these conditions still gave higher than acceptable background for any analysis to take place.

From this, we concluded that pre-treatment is not necessary for the chromosome spreads (see Materials and Methods).

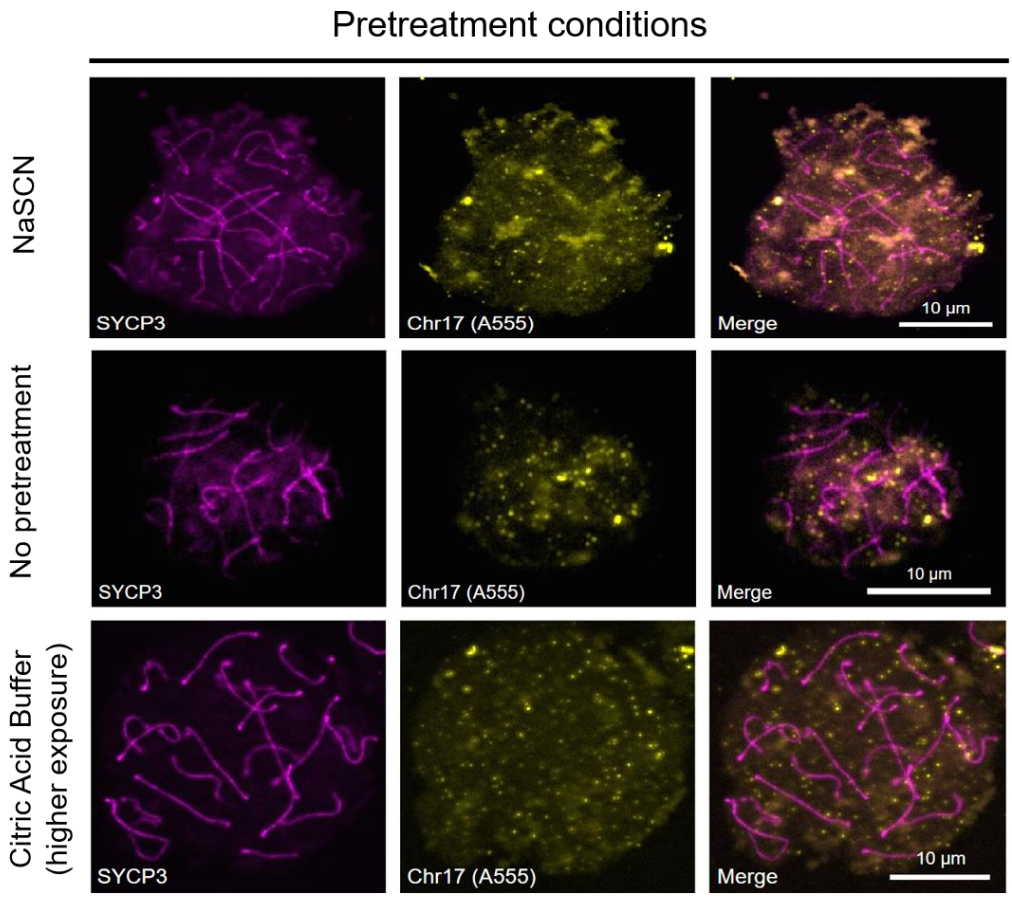

Figure 14: **Pachytene stages stained for SYCP3 and the probe hybridising to the hotspot on Chromosome 17.** The panel with cells without any pre-treatment shows a lesser background for the channel to visualise probes compared to the cells treated with citric acid buffer (CAB) and NaSCN. However, treatment with CAB gives background signal comparable to the condition without pre-treatment. Probe in yellow, and SYCP3 in Magenta.

3.4.3 Post-hybridisation washes

Once hybridisation is done, washing conditions are crucial to clean off unbound probes in order to reduce the background signal all the while keeping specifically bound probe. Ideal conditions had thus to be set up. We received a recommendation from Dr Sandrine le Noir (Laboratory CRIBL, France) to perform the washes at higher temperatures with a higher concentration of saline sodium citrate (SSC). For this condition, we first washed the slides in SSC 1X at 70°C, followed by one wash in SSC 1X at room temperature and

the last wash in SSC 0.05X at room temperature. This was tested on cells that had not been pre-treated before hybridisation, or using either NaSCN or CAB (data not shown). Unfortunately, this condition did not show any improvement in the probe signal.

However, when we performed the washing at a high temperature and high stringency of SSC (lower concentration), the signal for the probe improved drastically. Indeed, with these washing conditions, the signal was robust, with 3-4 foci showing in all the nuclei that were imaged. *(Figure 15).*

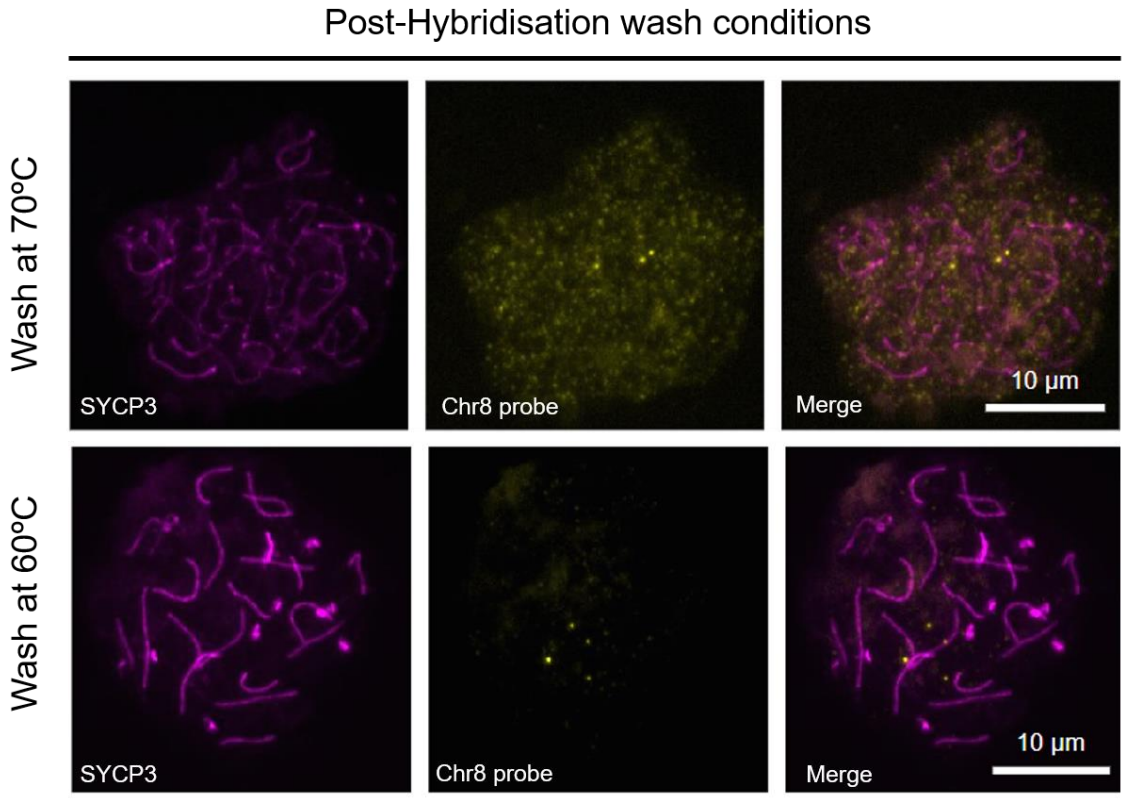

Figure 15: Pachytene cells SYCP3 and the probe hybridising to the hotspot on Chromosome 8. *Higher wash buffer stringency and higher temperature together are effective in washing away all the unbound probes or probes that were stuck non-specifically. SYCP3 is in Magenta, and the probe is in Yellow.*

This result also shows that both temperature and stringency need to be carefully balanced to achieve desired results, and one alone cannot get rid of all the background signals.

3.3.4 Pre-hybridisation and hybridisation

For better binding of probes to the target, we must ensure that both denatured single-stranded probes and single-stranded DNA (after denaturation) are present in close proximity and have ample time to bind to each other.

In our current protocol, we denature the probe and the chromatin separately and place them on ice before pouring the hybridization mixture (containing the probe) onto the slide. This has a disadvantage in that during handling the temperatures may rise, resulting in duplex formation even before the probe can bind to its target. In a protocol by Szabo et al., 2021, the denaturation was done in presence of the hybridisation mixture on the coverslip. After denaturation, the probe was allowed to hybridise for 12-14 hours between 37-52˚C. We thus decided to test denaturation in presence of the hybridisation mixture. Szabo et al., 2021 also perform the denaturation step at a lower temperature than in our protocol (78-80°C vs 85°C). Using a lower temperature could potentially be interesting for the preservation of the quality the immunofluorescence, as proteins tend to denature at high temperatures.

For denaturation to occur at a lower temperature, compared to the temperature that is used for PCR, the cells are treated with formamide, which is known to destabilise the DNA double helix structure and can unwind the DNA. Exploiting this property of formamide, the denaturation and the speed of renaturation can be changed. We thus tried two denaturing conditions. In the first condition, we treated the cells with a solution of 50% formamide and 50% SSC 2X for 20 minutes at room temperature, and then transferred the slides to a water bath set at 60°C for another 20 minutes before denaturing the chromatin on a heating block. In the second condition, we selected the same condition, except the chromatin and the probe were now denatured together. After treatment of the chromatin with 50% formamide and 50% SSC 2X for 20 minutes at 60°C,

the hybridization mixture was applied and sealed with rubber cement. After the rubber cement had dried, the entire slide was denatured at 85°C by placing on a heating block. Apart from trying these two conditions, I also tested two distinct hybridisation temperatures on the probe signal, 52°C and 55°C.

We can observe that increasing the hybridisation temperature from 52°C (Co-denaturation and prehybridization treatment) to 55°C does not have any effect on the robustness of the probe signal *(Figure 16).* However, the slight increase in the temperature had a considerable effect on the quality of MEI4 immunostaining (not shown). The protein had a poorer pattern compared to what is observed at lower temperatures. From this, we can say that the binding of the probe requires a threshold temperature (which seems to be achieved at 52°C), and above that temperature, the effect on binding does not change significantly, but MEI4 staining quality is greatly preserved at lower temperatures. However, the difference between co-denaturation and pre-hybridisation treatment were not strikingly different *(Figure 16).* They both had the expected number of foci (most of the time four per cell), and had almost no background signal. The same pattern of foci was observed at leptotene stage, something which was hard to observe in the prior tests. While neither of the conditions had too high background noise, it was observed that co-denaturation showed slightly better results in terms of background signal.

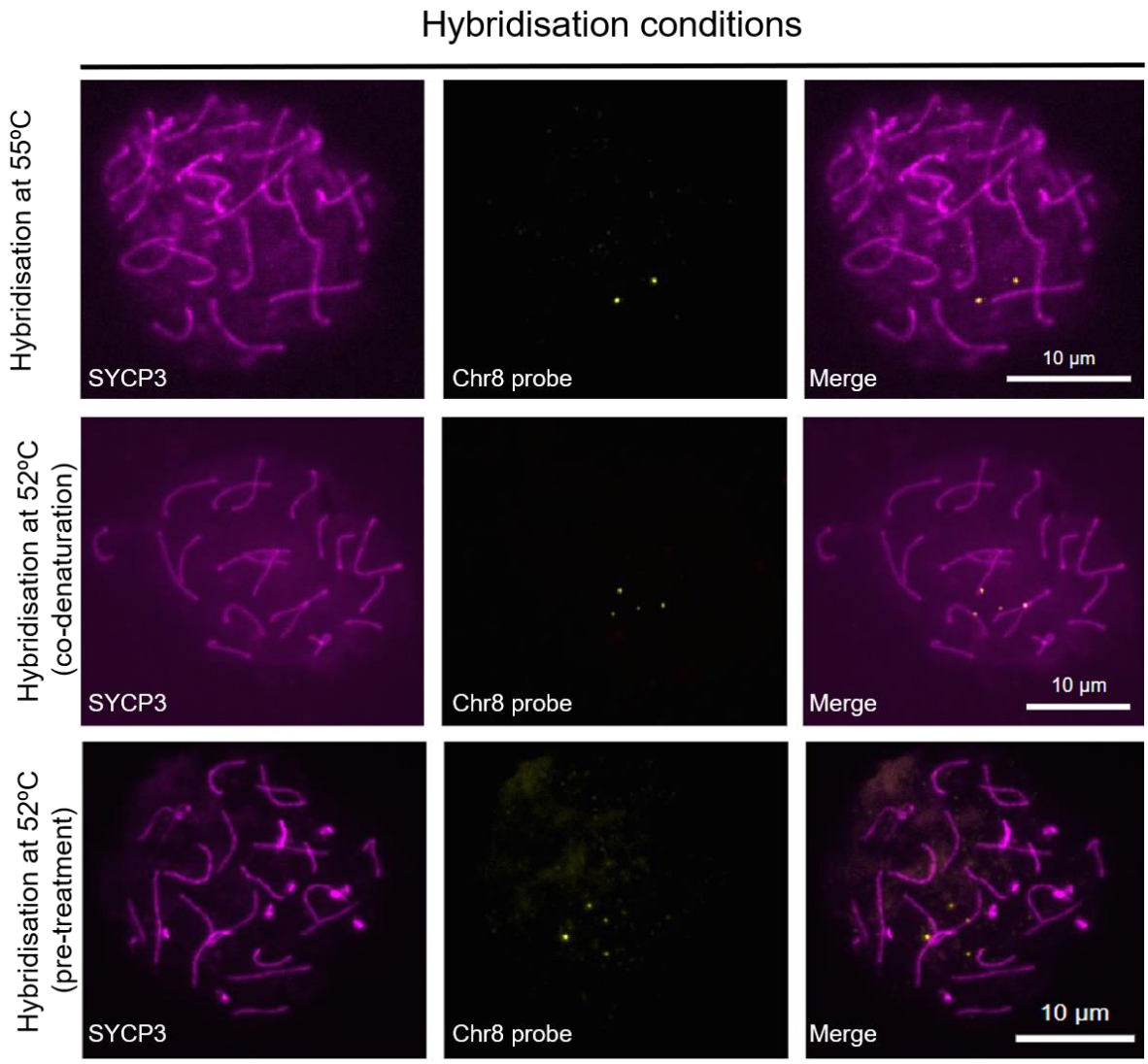

Figure 16: Pachytene cells stained for SYCP3 and probe hybridising to chromosome 8 tested under different parameters for hybridisation. *In all three panels, the probe shows up as 2-4 foci. This corresponds well with what is expected in the presence of four sister chromatids. The temperature for the cells that were co-denatured and those that were treated with formamide before hybridisation was 52°C, while in the top panel, the hybridization temperature was 55 °C*. Increasing the temperature for overnight (12 hours) hybridisation did not have an effect on the probe signal.

3.5 Conclusion for Part I:

Based on all the conditions that were tested in this study, it can be concluded that the post-hybridization wash had the most significant effect in reducing the background noise for probes. This is likely due to the high stringency of the wash buffer and the higher temperature at which washes were performed. The higher temperature likely opens up the helix slightly, and the low concentration of SSC (high stringency) is unable to shield the DNA double helix efficiently, which might result in the DNA probes not being bound tightly enough and can be washed away. Apart from this, pre-treating the cells to make the chromatin more accessible had no effect on the binding of probes, but with the treatment being carried out at temperatures between 70-80°C, it might be affecting MEI4 immunostaining. At last, the hybridisation temperature above a threshold did not affect the signal of the probe, but the prolonged exposure to high temperature decreased the signal of MEI4 protein.

We thus decided to move forward with the following workflow:

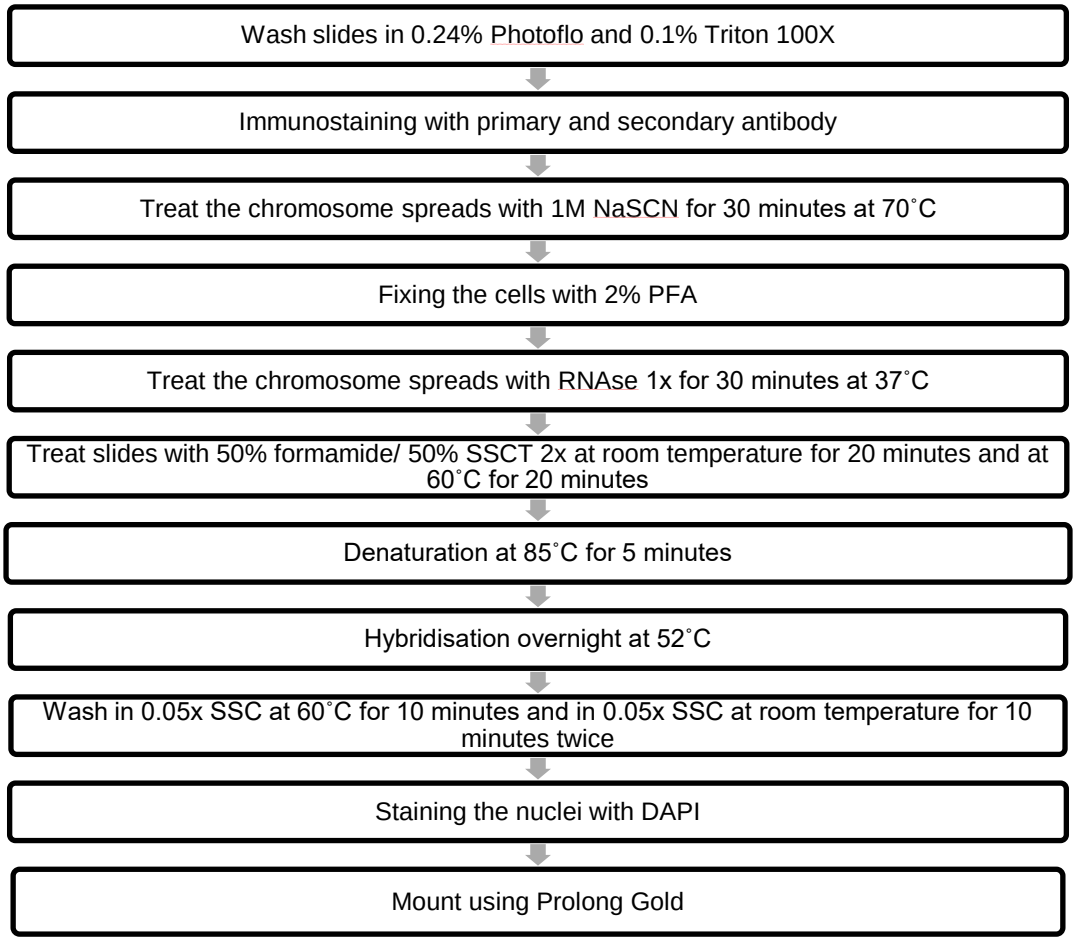

Figure 17: Workflow for the modified Immuno-FISH technique. *In the modified protocol, the order of the immunostaining and FISH was reversed so that the former is performed before FISH. After immunostaining, the spreads were fixed using 2% paraformaldehyde. Pre-treatment is no longer performed on the spreads before RNase treatment. The probe was then added and allowed to hybridise overnight. At last, the nuclei were stained with DAPI.*

Next, we still have to assess whether these conditions can also be adapted for the other probes we designed, notably the ones designed to bind at DSSBs. Once the protocol is set for all probes, probe specificity has to be assessed. The above probe only yields 1 to 4 foci per nucleus, which we interpret as being the same loci on four sister chromatids. However, to test if these loci are hybridizing to the right position, one of the perspectives is to perform whole chromosome paint at the same time as probe hybridization in order

to test whether the probes hybridize on the correct chromosomes. Moreover, staining at pachytene allows us to assess the approximate position within the chromosome depending on whether the probes bind at a proximal, central, or distal position. This data can be used to compare it to the expected binding position according to their genomic location. These tests will allow us to validate the probes I designed and proceed with the further analysis.

The first step of the analysis will consist in counting the number of foci for hotspot- and DDSB -probes in wild type vs *Prdm9KO* mice. Differences can be expected if hotspots are activated. It can be expected that sister chromatids would more often be in proximity when hotspots are used (wildtype) compared to when they are silent (*Prdm9KO*). The same experiment can be done for DDSB sites, with unknown predictions.

The second step will be to compare the overlap of hotspot- and DDSB- probes with MEI4 foci or with axis proteins in both genetic backgrounds. This will allow us to analyse whether hotspots tend to colocalize more often with the DSB machinery than DDSB sites in wild type and vice versa in *Prdm9KO*.

Third, co-staining of hotspots and DDSB with MEI4 foci will also be analysed by super resolution microscopy in order to detect possible differences. Setting up this Immuno-FISH protocol will thus pave the way to answer many longstanding questions concerning the relative behaviours of hotspots vs DDSB sites when PRDM9 is present or absent at the single cell level.

PART II

Recent studies have shown the interplay between the RMI proteins, MEI4 and IHO1, and hotspots (Biot et al., 2024). Biot et al. observed that the methyltransferase activity of PRDM9 was essential in recruiting MEI4 and IHO1 to PRDM9 sites. They also showed that IHO1 was necessary for the recruitment of the axis proteins HORMAD1 and SYCP3 to hotspots. However, this study did not shed any light on the localization of REC114, a crucial component of the RMI complex. Indeed, REC114 links the catalytic components of the DSB machinery (SPO11/TOPVIBL) to the RMI DSB-machinery (Nore et al. 2023). We expect that its localisation will follow the same pattern as that of MEI4 and will be enriched at the hotspots, but the relative genetic dependencies of its localisation remain unknown. To test the genomic localisation of REC114 in different mutant backgrounds compared to the wild type, we first had to test whether it is possible to perform a REC114 ChIP experiment with the available antibodies. For this purpose, we first had to select the right starting material. Indeed, ChIP experiments on meiotic proteins have proven to work only in testes where meiosis has been previously synchronised in order to enrich the leptotene/zygotene cell population.

4.1 Identifying the population of cells present in synchronised mouse testes

Since spermatogonia stem cells enter meiosis every 8-9 days, the cell population inside the testis contains cells in all different stages of meiosis. After the first round of successful meiosis, the majority of the cells found inside the testis are in pachytene, and very few cells are in leptotene and zygotene. This proves to be a problem if we want to extract any meaningful genomic information from the early stages of Prophase I, where the RMI proteins are highly enriched. To get around this, specific cell stages can be selectively enriched for by synchronising spermatogenesis with the introduction of retinoic acid. The protocol has been described in detail in Biot et al., 2024.

The synchronised testes were prepared by Mathilde Biot before I started on this project. However, before starting the ChIP experiment, I needed to assess the quality of

leptotene/zygotene enrichment by counting the average proportion of each meiotic stage present in the testis. This was done by immunostaining the chromosome spreads prepared from a thin section of the testis. The antibodies used were anti-SYCP1 and anti-SYCP3. SYCP1 is a component of the CE, which is gets associated to the axis as synapsis takes place. Based on the extent of staining for SYCP1, I classified the cells into early leptotene (EL), late leptotene/early zygotene (LL/EZ), and late zygotene (LZ) based on the number of fully synapsed axes present *(Figure 18).* For classification into the three different groups, I set the threshold and 5 and 9 fully synapsed axes. In EL, there were less than 5 axes which were completely synapsed. In LL/EZ, between 5-9 axes were completely synapsed, and in LZ, more than 9 axes which were completely synapsed. Once I verified the quality of the enrichment, the chromatin immunoprecipitation assay was performed.

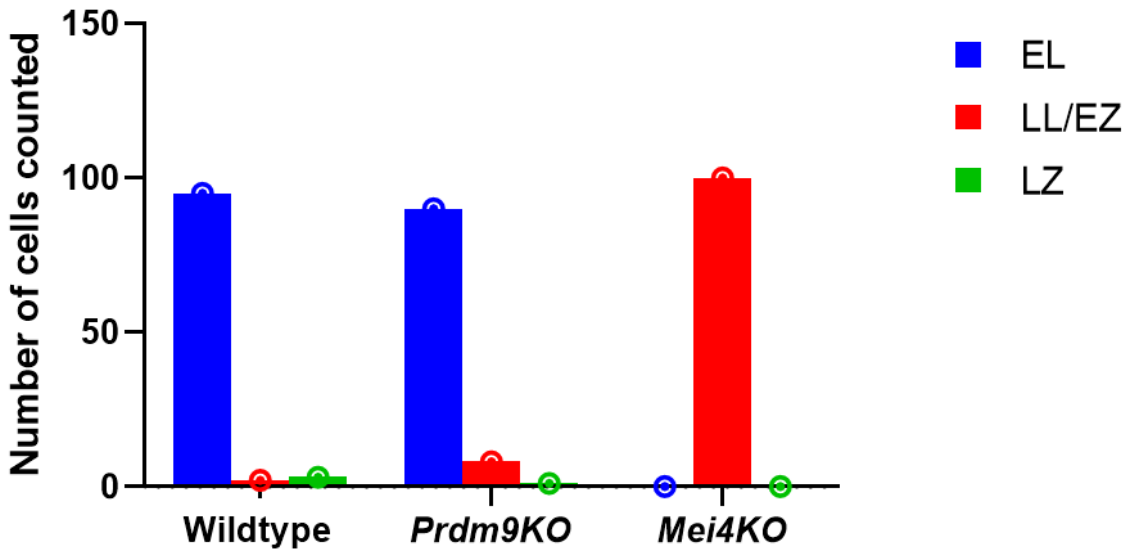

Figure 18: Relative abundance of the different germ cell stages present in the testis harvested from mice of different genotypes. *For all three genotypes, the early stages of prophase, i.e., leptotene and early zygotene, are enriched.*

4.2 Chromatin immunoprecipitation on synchronised mouse testis

We performed the ChIP experiment with antibodies anti-MEI4 and anti-REC114 on chromatin prepared from wildtype, *Prdm9KO* and *Mei4KO* mice. By analogy of what we observe for the other two RMI proteins (MEI4 and IHO1) (Biot et al., 2024), we expect REC114 to bind at hotspots in a PRDM9 dependent manner. Thus, at the tested hotspots, ChIP signal is expected in the wild type but not *Prdm9KO* mice. By immunofluorescence, in *Mei4KO* mice REC114 signal was strongly reduced (Kumar et al., 2018), testing its genomic localisation in *Mei4KO*, will allow to determine if this reduction reflects its binding on hotspots.

First, I checked if the antibody is compatible with the conditions under which ChIP will be carried out. This was done by performing IP on the crosslinked chromatin with REC114, and later revealing the protein using Western Blotting (WB*) (Figure 19).* To make sure that the result was not overshadowed by the signal of the IgG that would come up if an antibody from the same host is used for both IP and WB, the antibody used for WB was chosen to be chicken anti-REC114. I could detect two bands: one band was at around 50 kDa which indicates that the anti-chicken HRP recognized non-specifically the heavy chain of rabbit IgG, and the other was close to 30 kDa, which was the expected size of REC114 protein. However, the signal was very faint. We concluded that the anti-REC114 antibody could be potentially used in the ChIP protocol with the risk of retrieving only weak signal.

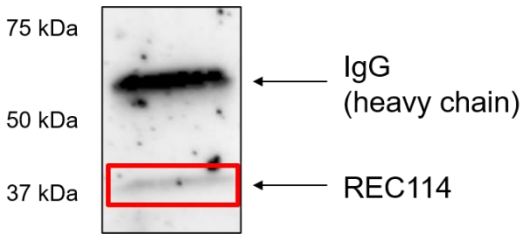

Figure 19: Western blot image from wildtype mouse crosslinked chromatin showing the band for REC114 protein close to 30 kDa. *The IP was performed with rabbit anti-REC114 and WB with chicken anti-REC114.*

After the antibodies were validated for the ChIP protocol, we performed a ChIP experiment on wild type testes. As a positive control, we also performed a ChIP with anti-MEI4 antibody, which has previously been shown to yield robust enrichment at hotspots (Biot et al., 2024). After ChIP, we assessed the enrichment of MEI4 and REC114 bound fragments by quantitative PCR (qPCR). We used primers for hotspots active in C57BL/6 mice, *Pbx1* hotspot and another hotspot on chromosome 14 (14A), and one control region *Hlx1.6* (not active in C57BL/6 mice) in both wildtype and corresponding knockout strains. The fold enrichment for MEI4 binding for these hotspots and the control site (*Hlx1.6*) are known. In the study by Biot et al., they found the enrichment of MEI4 at hotspot *Pbx1a* to be 5-7 times enriched compared to the coldspot *Hlx1.6.* Here, we also report the same observation; MEI4 is about 5 times enriched at the hotspot *Pbx1a (Figure 20).* Next, we found that REC114 enrichment at the *Pbx1* hotspot is approximately 30 times higher in comparison to the control site *Hlx1.6* (Figure 18). The same trend was observed for the hotspot on chromosome 14 with 33 times enrichment of REC114 in the wildtype. However, in *Prdm9KO* and *MEI4KO* mice, no enrichment was observed for either MEI4 or REC114 *(Figure 20).*

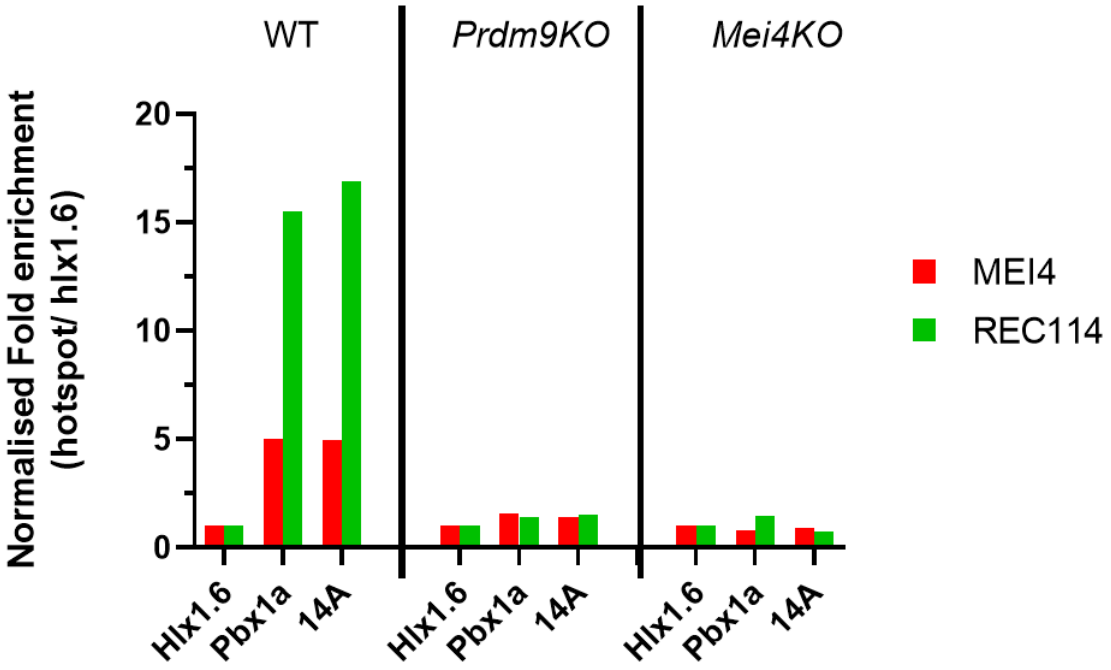

Figure 20: REC114 and MEI4 enrichment at the hotspots by qPCR. *The experiment has been performed on sheared chromatin from synchronised testes. Data shown is from a single experiment.*

4.3 Conclusion for Part II:

We observe from the data from qPCR that REC114 follows the same localisation pattern as MEI4, which aligns with our expectations since the proteins are present in a complex. In *Mei4KO*, there is no enrichment of REC114, which can mean that REC114 is recruited downstream of MEI4 recruitment. In *Prdm9KO,* neither protein is enriched, and this can be explained by the fact that no breaks are forming in these hotspot regions anymore. However, to arrive at a stronger conclusion, this experiment needs to be repeated to obtain more data.

General Conclusion

By the end of this study, I have been able to set up the Immuno-FISH protocol which enables us to look at the hotspots or the DDSBs, the RMI proteins and the axis proteins simultaneously. This will allow us to track the spatiotemporal dynamics of PRDM9-dependent hotspots and PRDM9-independent DDSB sites relative to the DSB-machinery protein MEI4 at the single-cell level. Specifically, we can now start looking at the overlap of hotspot and DDSB probes with MEI4 foci or axis proteins in both wildtype and *PRDM9KO* backgrounds. Additionally, we can detect any possible differences of hotspots and DDSB with MEI4 foci by super resolution microscopy.

In the second part of my project, I have shown a preliminary data for REC114 enrichment at hotspots in a C57BL/6 mouse. Still, quite a lot of work remains to be done to answer the questions that we had started with to establish its genomic localisation (hotspot or DDSB site). Once that is established, we can test the conditions required for the recruitment of REC114 to these sites, such as, the presence of MEI4, the catalytic activity of PRDM9 etc.

In the last seven months, I have learnt how to optimise a protocol and how sample variation has to be taken into account. It helped me to analyse the result of each test critically, and to remove any sort of bias that would lead to skewed conclusions. Even for protocols that are well established, caution needs to be taken when adapting it to a different system of organism. Another lesson on accuracy and precision came while preparing the samples for qPCR. Even for volumes small enough to be indistinguishable to the human eye, it can lead to really drastic outcomes when values are rising exponentially, I this learnt to work very carefully in order to obtain reproducible results.

Apart from the experiments, I gained a lot of theoretical knowledge through the lab meetings, scientific discussion, journal club meetings, conferences and seminars etc.

Through engaging in these discussions, my curiosity was kept alive and I was constantly learning something new every day. I also realised the importance of planning my weekly experiments and strived to complete everything within a set timeframe.

References

Acquaviva, L., Drogat, J., Dehé, P. M., de La Roche Saint-André, C., & Géli, V. (2013). Spp1 at the crossroads of H3K4me3 regulation and meiotic recombination. Epigenetics, 8(4), 355–360. https://doi.org/10.4161/epi.24295

Baudat, F., Buard, J., Grey, C., Fledel-Alon, A., Ober, C., Przeworski, M., Coop, G., & de Massy, B. (2010). PRDM9 is a major determinant of meiotic recombination hotspots in humans and mice. Science (New York, N.Y.), 327(5967), 836–840. https://doi.org/10.1126/science.1183439

Bergerat, A., de Massy, B., Gadelle, D., Varoutas, P.-C., Nicolas, A., and Forterre, P. (1997). An atypical topoisomerase II from archaea with implications for meiotic recombination. Nature 386, 414–417.

Borde V. (2007). The multiple roles of the Mre11 complex for meiotic recombination. *Chromosome research : an international journal on the molecular, supramolecular and evolutionary aspects of chromosome biology*, *15*(5), 551–563. https://doi.org/10.1007/s10577-007-1147-9

Borde, V., Robine, N., Lin, W., Bonfils, S., Géli, V., & Nicolas, A. (2009). Histone H3 lysine 4 trimethylation marks meiotic recombination initiation sites. *The EMBO journal*, *28*(2), 99–111. https://doi.org/10.1038/emboj.2008.257

Brick, K., Smagulova, F., Khil, P., Camerini-Otero, R. D., & Petukhova, G. V. (2012). Genetic recombination is directed away from functional genomic elements in mice. *Nature*, *485*(7400), 642–645. https://doi.org/10.1038/nature11089

Cromie, G., & Smith, G. R. (2008). Meiotic Recombination in Schizosaccharomyces pombe: A Paradigm for Genetic and Molecular Analysis. *Genome dynamics and stability*, *3*, 195. https://doi.org/10.1007/7050_2007_025

Diagouraga, B., Clément, J. A. J., Duret, L., Kadlec, J., de Massy, B., & Baudat, F. (2018). PRDM9 Methyltransferase Activity Is Essential for Meiotic DNA Double-Strand Break Formation at Its Binding Sites. *Molecular cell*, *69*(5), 853–865.e6. https://doi.org/10.1016/j.molcel.2018.01.033

Grey, C., & de Massy, B. (2021). Chromosome Organization in Early Meiotic Prophase. *Frontiers in cell and developmental biology*, *9*, 688878. https://doi.org/10.3389/fcell.2021.688878

Hunter N. (2015). Meiotic Recombination: The Essence of Heredity. *Cold Spring Harbor perspectives in biology*, *7*(12), a016618. https://doi.org/10.1101/cshperspect.a016618

Kauppi, L., Barchi, M., Baudat, F., Romanienko, P. J., Keeney, S., & Jasin, M. (2011). Distinct properties of the XY pseudoautosomal region crucial for male meiosis. *Science (New York, N.Y.)*, *331*(6019), 916–920. https://doi.org/10.1126/science.1195774

Keeney, S., Giroux, C. N., & Kleckner, N. (1997). Meiosis-specific DNA double-strand breaks are catalyzed by Spo11, a member of a widely conserved protein family. *Cell*, *88*(3), 375–384. https://doi.org/10.1016/s0092-8674(00)81876-0

Keeney S. (2001). Mechanism and control of meiotic recombination initiation. *Current topics in developmental biology*, *52*, 1–53. https://doi.org/10.1016/s0070-2153(01)52008-6

Khil, P. P., Smagulova, F., Brick, K. M., Camerini-Otero, R. D., & Petukhova, G. V. (2012). Sensitive mapping of recombination hotspots using sequencing-based detection of ssDNA. *Genome research*, *22*(5), 957–965. https://doi.org/10.1101/gr.130583.111

Kumar, R., Bourbon, H. M., & de Massy, B. (2010). Functional conservation of Mei4 for meiotic DNA double-strand break formation from yeasts to mice. *Genes & development*, *24*(12), 1266–1280. https://doi.org/10.1101/gad.571710

Kumar, R., & De Massy, B. (2010). Initiation of meiotic recombination in mammals. *Genes*, *1*(3), 521–549. https://doi.org/10.3390/genes1030521

Kumar, R., Oliver, C., Brun, C., Juarez-Martinez, A. B., Tarabay, Y., Kadlec, J., & de Massy, B. (2018). Mouse REC114 is essential for meiotic DNA double-strand break formation and forms a complex with MEI4. *Life science alliance*, *1*(6), e201800259. https://doi.org/10.26508/lsa.201800259

Lam, I., & Keeney, S. (2015). Nonparadoxical evolutionary stability of the recombination initiation landscape in yeast. *Science (New York, N.Y.)*, *350*(6263), 932–937. https://doi.org/10.1126/science.aad0814

Laroussi, H., Juarez-Martinez, A. B., Le Roy, A., Boeri Erba, E., Gabel, F., de Massy, B., & Kadlec, J. (2023). Characterization of the REC114-MEI4-IHO1 complex regulating meiotic DNA double-strand break formation. *The EMBO journal*, *42*(16), e113866. https://doi.org/10.15252/embj.2023113866

Li, W., Ma, H. Double-stranded DNA breaks and gene functions in recombination and meiosis. *Cell Res* 16, 402–412 (2006). https://doi.org/10.1038/sj.cr.7310052

Lorenz, A., Wells, J. L., Pryce, D. W., Novatchkova, M., Eisenhaber, F., McFarlane, R. J., et al. (2004). S. pombe meiotic linear elements contain proteins related to synaptonemal complex components. J. Cell. Sci. 117, 3343–3351. doi: 10.1242/ jcs.01203

Mihola, O., Pratto, F., Brick, K., Linhartova, E., Kobets, T., Flachs, P., Baker, C. L., Sedlacek, R., Paigen, K., Petkov, P. M., Camerini-Otero, R. D., & Trachtulec, Z. (2019). Histone methyltransferase PRDM9 is not essential for meiosis in male mice. *Genome research*, *29*(7), 1078–1086. https://doi.org/10.1101/gr.244426.118

Morelli, M. A., Werling, U., Edelmann, W., Roberson, M. S., & Cohen, P. E. (2008). Analysis of meiotic prophase I in live mouse spermatocytes. *Chromosome research : an international journal on the molecular, supramolecular and evolutionary aspects of chromosome biology*, *16*(5), 743–760. https://doi.org/10.1007/s10577-008-1224-8

Muller, H., Scolari, V. F., Agier, N., Piazza, A., Thierry, A., Mercy, G., Descorps-Declere, S., Lazar-Stefanita, L., Espeli, O., Llorente, B., Fischer, G., Mozziconacci, J., & Koszul, R. (2018). Characterizing meiotic chromosomes' structure and pairing using a designer sequence optimized for Hi-C. *Molecular systems biology*, *14*(7), e8293. https://doi.org/10.15252/msb.20188293

Nasmyth K, Haering CH. Cohesin: its roles and mechanisms. Annu Rev Genet. 2009;43:525-558. doi:10.1146/annurev-genet-102108-134233

Page, S. L., & Hawley, R. S. (2004). The genetics and molecular biology of the synaptonemal complex. *Annual review of cell and developmental biology*, *20*, 525–558. https://doi.org/10.1146/annurev.cellbio.19.111301.155141

Panizza, S., Mendoza, M. A., Berlinger, M., Huang, L., Nicolas, A., Shirahige, K., & Klein, F. (2011). Spo11-accessory proteins link double-strand break sites to the chromosome axis in early meiotic recombination. *Cell*, *146*(3), 372–383. https://doi.org/10.1016/j.cell.2011.07.003

Peters, A. H., Plug, A. W., van Vugt, M. J., & de Boer, P. (1997). A drying-down technique for the spreading of mammalian meiocytes from the male and female germline. *Chromosome research : an international journal on the molecular, supramolecular and evolutionary aspects of chromosome biology*, *5*(1), 66–68. https://doi.org/10.1023/a:1018445520117

Peters JM, Tedeschi A, Schmitz J. The cohesin complex and its roles in chromosome biology. Genes Dev. 2008;22(22):3089-3114. doi:10.1101/gad.1724308

Petronczki, M., Siomos, M. F., & Nasmyth, K. (2003). Un ménage à quatre: the molecular biology of chromosome segregation in meiosis. *Cell*, *112*(4), 423–440. https://doi.org/10.1016/s0092-8674(03)00083-7

Robert, T., Nore, A., Brun, C., Maffre, C., Crimi, B., Bourbon, H. M., & de Massy, B. (2016). The TopoVIB-Like protein family is required for meiotic DNA double-strand break formation. *Science (New York, N.Y.)*, *351*(6276), 943–949. https://doi.org/10.1126/science.aad5309

Sommermeyer, V., Béneut, C., Chaplais, E., Serrentino, M. E., & Borde, V. (2013). Spp1, a member of the Set1 Complex, promotes meiotic DSB formation in promoters by tethering histone H3K4 methylation sites to chromosome axes. *Molecular cell*, *49*(1), 43–54. https://doi.org/10.1016/j.molcel.2012.11.008

Stanzione, M., Baumann, M., Papanikos, F., Dereli, I., Lange, J., Ramlal, A., Tränkner, D., Shibuya, H., de Massy, B., Watanabe, Y., Jasin, M., Keeney, S., & Tóth, A. (2016). Meiotic DNA break formation requires the unsynapsed chromosome axis-binding protein IHO1 (CCDC36) in mice. *Nature cell biology*, *18*(11), 1208–1220. https://doi.org/10.1038/ncb3417

Yamada, S., Ohta, K., & Yamada, T. (2013). Acetylated Histone H3K9 is associated with meiotic recombination hotspots, and plays a role in recombination redundantly with other factors including the H3K4 methylase Set1 in fission yeast. *Nucleic acids research*, *41*(6), 3504–3517. https://doi.org/10.1093/nar/gkt049

Zickler, D., & Kleckner, N. (1999). Meiotic chromosomes: integrating structure and function. *Annual review of genetics*, *33*, 603–754. https://doi.org/10.1146/annurev.genet.33.1.603

Zickler, D., & Kleckner, N. (2015). Recombination, Pairing, and Synapsis of Homologs during Meiosis. *Cold Spring Harbor perspectives in biology*, *7*(6), a016626. https://doi.org/10.1101/cshperspect.a016626

Supplementary Data

Table S1: Primers used for amplifying the region of interest and making the probes

Primer Name	**Primer Sequence**
Chr8_FP_1_F	TGGAATGCTGGAGTTTAGGG
Chr8_FP_1_R	CCGGGAATCATTGTTATTGG
Chr8_FP_2_F	TGCAAAGCACACAAGCAGA
Chr8_FP_2_R	TCCCGAGACCATCAAACAA
Chr8_FP_3_F	GAAAGCAGGGAAAAGCACA
Chr8_FP_3_R	ATCAATTCCAGGTGGCAGA
Chr8_FP_4_F	TAAAGGCTTTTCCGGATGG
Chr8_FP_4_R	TGTGCTGATTTGTTGGTGCT
Chr8_FP_5_F	CCCAAGTCTCACCACAAACA
Chr8_FP_5_R	AAGGGCACACGAGATGAAA
Chr8_FP_6_F	ACTCCTGCCAGAAATGGATG
Chr8_FP_6_R	TTACCCTGCCACAGTTTTCC
Chr8_FP_7_F	TGCTCCCAAACTATCCCTGT
Chr8_FP_7_R	GATGCAACCAGGCAGAAAA
Chr17_FP_1_F	CCATGGAAGAAGACCAGGAA
Chr17_FP_1_R	TCAGTTGCACAGTAAGGACCAC
Chr17_FP_2_F	AGGGCTTCTTTGAGATGCTG

Chr17_FP_2_R	TTTCAAAGAGACCAGGCAAAA
Chr17_FP_3_F	AGGCAAGTCCCTTTCATCCT
Chr17_FP_3_R	CGGCTTGGCTGTGTTTTT
Chr17_FP_4_F	AGGTGCCAAGGTGCAATAAC
Chr17_FP_4_R	TGAGGCCACCAGCAATAAA
Chr17_FP_5_F	TGACATTTCTGAATCTTTTGGA
Chr17_FP_5_R	TTACCTGTGCCCTCTGATTT
Chr17_FP_6_F	TGCTTAGATGGAATGCTTGG
Chr17_FP_6_R	TTCTCTGGGGTATTCCCTTTT
Chr17_FP_7_F	TTTGTTGGCAGGTGTGTTG
Chr17_FP_7_R	ACCCAGGCGTAAAAGGTAGA
Chr17_FP_8_F	AACCATCCGCCATAAGGAA
Chr17_FP_8_R	TAGCCACCCTATGAGATTCAGG
Chr6_FP_1_F	TCATGGTTTGCAGGTATTGG
Chr6_FP_1_R	ATTGAGGGTGATGAGGGTTG
Chr6_FP_2_F	ATACAATGCTACGGGTCTCTCC
Chr6_FP_2_R	CGCTGGAGCATCAAATCA
Chr6_FP_3_F	CATGGGATTCCTTTTCTCCTC
Chr6_FP_3_R	TTTCTACCCCCTCCCTGTTT
Chr6_FP_4_F	TGAATTTGGCCTGAAAGGA
Chr6_FP_4_R	GAGCAGTGGGCACAAATAGA

Chr6_FP_5_F	TTTTACAGCGCATTCAGCAC
Chr6_FP_5_R	GAACGCCAGTTCCATTTCA
Chr6_FP_6_F	CTCACACAAATCCCATTCCA
Chr6_FP_6_R	TGGAAAAGCCATACCCTTGT
Chr6_FP_7_F	AGGCAGCCAAAATGAAAGG
Chr6_FP_7_R	CAAACTTCTGTGCTGGGTGA
Chr6_FP_8_F	AGAATGATCTGCCACACGA
Chr6_FP_8_R	AGCTGAGACTTTCTTGGCTCT
Chr4_FP_1_F	AAGGTTCAGATCATTCCTGTCC
Chr4_FP_1_R	TAACTCGGACCCGCTATTTC
Chr4_FP_2_F	TGGCAGAAACAGAAGCACA
Chr4_FP_2_R	CAGAGGCGGCACTTAGTTTT
Chr4_FP_3_F	GGCATTGCAGAAGCAGAAA
Chr4_FP_3_R	GGCAGCCTGTGAAACAAAA
Chr4_FP_4_F	AGCAAATGCCCATGAATACC
Chr4_FP_4_R	AAATGCTACAAAGCCTGCTGA
Chr4_FP_5_F	TGGAAACCAGATGAACAGCA
Chr4_FP_5_R	AAGAGCCAGAGGTGAATGGA
Chr4_FP_6_F	CATTGTTGAGGCACATGGA
Chr4_FP_6_R	AATTGCCTGGCTCTGTTCTT
Chr4_FP_7_F	GCTGAGATTCCTTTGCGTCT

Chr4_FP_7_R	TTGGGCTCATGTTGTGGTT
Chr4_FP_8_F	TGGTGTTTCTTCAGCCTTGT
Chr4_FP_8_R	CTTAAATAGGCCTTGTGGAATG